ABSTRACT

Interference cancelation has been mainly performed using arrays, in an important issue in communication both array and spatial cancelation and time domain approach were used. In array applications, depth of cancelation may dependent on the interferences to background power ratio and their spatial distributions. Also, array cancelers are inadequate when the signals are less than an array beamwidth apart. The latter was dealt with using supperesolution and eigenanalysis methods. Different time domain methods were used in the past. Among them what is termed Cross-Coupled PLL. It is an arrangement of two PLL each one is locked on and tracking one signal of the two at the input. In fact the output of such a system is dependent on one signal or the other. In a way Cross-Coupled PLL is a signal separator. For the case of more than two signals we proposed in this thesis the N-Cross Coupled PLL. It is used to receive and process one of the N signals while suppressing the others which could be looked upon as interchannel interference. N-Cross Coupled PLLs consist of N PLLs interconnected using amplitude control loops that estimate the instantaneous amplitude of each signal. N-1 signals are then subtracted from the input to leave, as clear as possible, one signal to be handled by the corresponding PLL. If the PLLs are used as FM demodulators then we get at the output the information contained in each signal regardless of the signal's relative powers and or their modulation content. Thus N-Cross Coupled PLLs behave as N signals separator.

2) # N-Cross Coupled Phase Locked Loops

by

1) Joseph C. Aboukhalil

Thesis submitted to the Faculty of the Graduate School of
the New Jersey Institute of Technology in partial fulfillment of
the requirements for the degree of
Master of Science in Electrical Engineering

APPROVAL SHEET

Title of Thesis: N-Cross Coupled Phase Locked Loops

Name of Candidate: Joseph C. Aboukhalil
Master of Science in Electrical Engineering, 1991

Thesis and Abstract Approved: ______________________ __________

Dr. Y. Bar-Ness Date
Professor
Department of Electrical Engineering

______________________ __________

Dr. Chung H. Lu Date
Associate Professor
Department of Electrical Engineering

______________________ __________

Dr. Erdal Panayirci Date
Visiting Professor
Department of Electrical Engineering

VITA

Name: Joseph C. Aboukhalil.

Degree and date to be conferred: Master of Science in Electrical Engineering, 1991.

Secondary education: College Mont LaSalle, Ain Saade, Lebanon.

Collegiate institutions attended	Dates	Degree	Date of Degree
N. J. Institute of Technology	9/89-12/90	M.S.E.E.	January 1991
N. J. Institute of Technology	1/86-10/89	B.S.E.E.	October 1989
Jersey City State College	1/85-12/85		
Cuyahoga Community College	10/84-12/84		

Major: Electrical Engineering.

To my Parents.
my Sisters, Brothers and their Families.

Acknowledgment

This work would not have been possible if it had not been for Dr. Yeheskel Bar-Ness. His constant questioning and constructive criticism made this work and my education more than it would have been without him. I have learned a great deal from him.

I am grateful to Dr. Chung H. Lu and Dr. Erdal Panayirci for their effort and time in reviewing this work. Their comments helped to clarify some difficult concepts in the body of the text.

I would like to thank Dr. Stanley Reisman, Christopher Peckham, and Raafat Kamel for their help with BOSS and computers in general.

I would like to thank Karin S. Bannier for her emotional and constant support. She has patiently listened to all the problems I had during this work. And she gave me a lot of confidence.

Even if they have the dedication I want to thank Mom and Dad for sending me out of Lebanon so I could get more out of life.

Contents

List of Figures

Chapter 1

INTRODUCTION

1.1 Phase Locked Loops

1.1.1 History

In the year 1932, a group of British scientists experimented with a receiver simpler than the superheterodyne receiver. They wanted to reduce the number of tuned stages. The new method had to outperform the superheterodyne in order to receive recognition. The so called homodyne, and later synchrodyne, receiver, consisted of a local oscillator, a mixer, and an audio amplifier. Synchronization, however, was difficult because of the local oscillator's drift in frequency. A phase detector was then added to compare the output of the oscillator with the input signal. Thus a correction signal for the oscillator was found. It was not until the fourties that phase locked loops (PLLs) were widely used in television receivers. Today PLLs are used in almost every communication system (*e.g.* AM, PM and FM demodulators, FSK decoders, frequency synthesis, radar, telemetry, command, control, ranging,

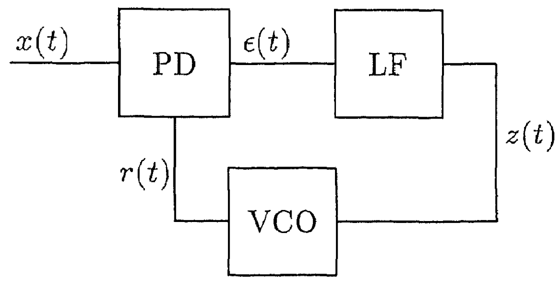

Figure 1.1: Block diagram of a Phase Locked Loop

and instrumentation systems).[1]

1.1.2 General PLL

One of the biggest problems in communication is transmission power. Since transmission power is somewhat limited (weight, power supply, price, or international power radiation regulations) the transmitted signals are often immersed in noise and more importantly in interference. In such cases traditional reception techniques are useless, but coherent detection is efficient.

A PLL is a device designed to lock on and follow the phase of an input. A PLL consists of three main blocks, a phase detector, a loop filter, and a voltage controlled variable frequency oscillator. (Fig. 1.1)

The output of the VCO (reference signal) is desired to be a good estimate of the input signal in frequency and phase. The two signals are then fed into a phase detector whose output is a function of their phase difference plus a higher frequency component. The latter is eliminated by the low pass loop filter, and the former, (*e.g.* error signal), serves as an error voltage for the VCO. This error voltage controls the change in the instantaneous frequency and phase of the reference signal.

1.1.3 Terminology

It will be helpful to become familiar with some basic terms before discussing PLLs. A PLL operates in one of two modes. The first is called the *acquisition mode* and it is the state of the loop when its reference signal has not yet started to follow the input signal. In other words it is the state when the loop is trying to achieve synchronization. The second mode is called the *tracking mode* and it is the state of the loop when the reference signal is continuously close to the input signal within a small phase error, or when the loop is in constant synchronization. *Sync failure* is the process of loosing lock, after the loop was in the tracking mode. *Cycle slipping* is the phenomenon when the reference signal either loses or gains one complete cycle (360°, or 2π).

The order of a PLL is determined by the number of poles at zero of the loop filter plus 1. The addition of one takes into account the pole of the VCO. The *pull-in range* is the maximum value of the difference in initial frequency from which the loop can reach the tracking mode. The signal *acquisition time*, or pull-in time, or lock-in time, is the time needed for the loop to reach the tracking mode after being in acquisition mode. And last but not least, PLLs have what is known as the capture effect.[2] This phenomenon describes the capability of a phase locked loop to lock on the strongest of signals if a number of inputs is applied.

1.1.4 General Equations

The general equations governing the operation of a PLL in a noiseless environment will be developed in this section. Assuming that:

$$s(t) = A \sin \phi(t) \tag{1.1}$$

$$r(t) = K_1 \cos \hat{\phi}(t) \tag{1.2}$$

where $\phi(t)$ and $\hat{\phi}(t)$ are,

$$\phi(t) = \omega_0 t + \theta(t)$$

$$\hat{\phi}(t) = \omega_0 t + \hat{\theta}(t)$$

Hence the output of the phase detector $\epsilon(t)$ is the product of its two inputs,

$$\epsilon(t) = s(t)r(t) = AK_1K_m \sin \Phi(t) + \text{double freq. term} \tag{1.3}$$

where,

$$\Phi(t) = \phi(t) - \hat{\phi}(t) \tag{1.4}$$

and K_m is the phase detector gain.

After the loop filter, $f(t)$, which is a low pass, the double frequency term can be neglected and the input to the VCO z(t) is,

$$\begin{aligned} z(t) &= \epsilon(t) * f(t) \\ &= \int_{-\infty}^{\infty} \epsilon(\tau) f(t-\tau) d\tau \end{aligned} \tag{1.5}$$

where * is the convolution. Since the VCO is an oscillator whose frequency is modulated by its input, with a modulation sensitivity K_v in rad/s/V, then,

$$\frac{d\hat{\phi}(t)}{dt} = K_v z(t) \tag{1.6}$$

$$\frac{d\hat{\phi}(t)}{dt} = AK_1K_mK_v\sin(\Phi(t)) * f(t) \tag{1.7}$$

$$\frac{d\hat{\phi}(t)}{dt} = AK\sin(\Phi(t)) * f(t)$$

$$\frac{d\hat{\phi}(t)}{dt} = AK\sin(\phi(t) - \hat{\phi}(t)) * f(t) \tag{1.8}$$

where $K = K_1K_mK_v$ and is known as the open loop gain. Chapter 2 will discuss some of the applications of PLLs as well as the loop equations in both noisy and noiseless environments.

1.2 Cross Coupled Phase Locked Loops (CC-PLL)

In this section, the basic theory behind CCPLLs (2CCPLL)[3] as an FM demodulator will be introduced. The CCPLL is capable of seperating and demodulating two signals even if they have the same center frequency. The scheme makes use of the capture effect of a PLL.

CCPLL (see figure 1.2) consists of two PLLs connected together in such a manner to help suppress interchannel and cochannel interference. One of the two PLLs locks onto and tracks the stronger of the two signals, and through the interconnection helps the other lock onto and track the weaker signal. Furthermore, each PLL is capable of performing FM demodulation on one of the two signals.

The CCPLL tracking behavior is the same as that of a PLL. Because of the the two signals at the input, the acquisition behavior is different from that of the single PLL. At the input of both adders in Figure 1.2, the signal is composed of

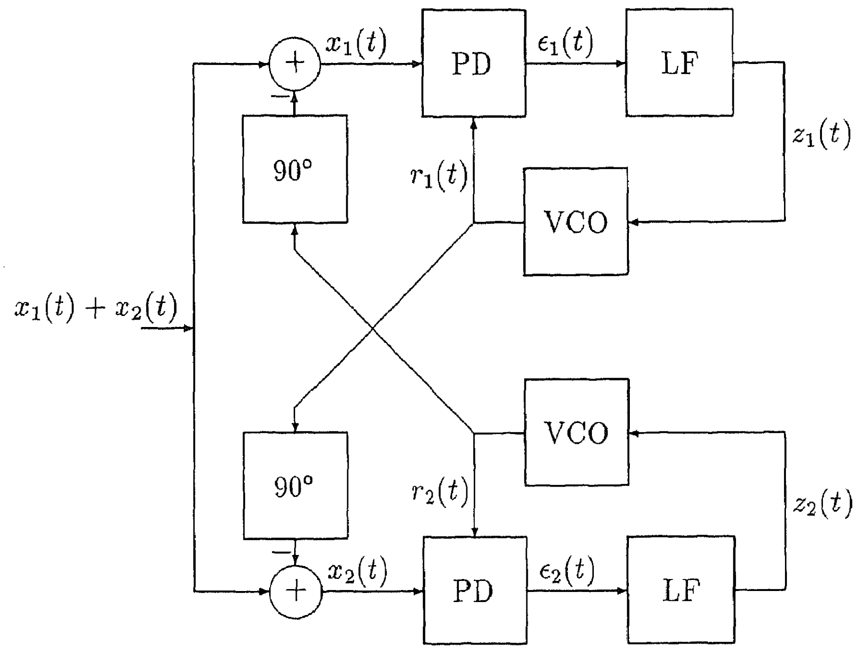

Figure 1.2: Block Diagram of a CCPLL

two independent signals $x_1(t)$ and $x_2(t)$. In steady state, only one signal will be present at the output of each adder. Let us assume that one of the signals, say $x_1(t)$, is larger (even slightly) than the other, $x_2(t)$. Because of the capture effect, it is reasonable to assume that loop 1 will lock on $x_1(t)$. It is well known that the VCO output, $r_1(t)$, is 90° behind its input, so the other 90° results in 180° phase shift. The adder of loop 2 will subtract $x_1(t)$ from the input signal leaving only $x_2(t)$ as an input to the second loop. In a similar manner, the adder of loop 1 will subtract $x_2(t)$ from the input signal insuring that only $x_1(t)$ is applied to loop 1. It does not matter which loop is tracking which signal. It is sufficient to recognize the desired output to determine which loop it is. Since the amplitude of the VCO is not related to the amplitude of the signal input to the loop, this scheme will need an amplitude control system to make sure that the signals are subtracted in the right amount.

This system, including the amplitude control, is discussed in chapter 3. Also, chapter 3 will present the N-cross coupled PLL (NCCPLL) and its mathematical model. Chapter 4 will particularly outline the 3CCPLL example. Chapter 5 contains results and conclusions.

Chapter 2

Phase Locked Loops

The PLL model described in chapter 1 contains the basic form, or the essential building block of a PLL. The block diagram in figure 2.1 is a more general model for a PLL as it applies to AM, PM and FM demodulation[4]. The following is a list of keys for the figure:

- PD = Phase detector
- LF = Loop filter
- OF = Output filter
- 90° PS = A 90° phase shifter
- WG = The waveform generator that needs synchronization. Either a VCO or an FCO
- AA = Acquisition aid
- AGC = Coherent automatic gain control

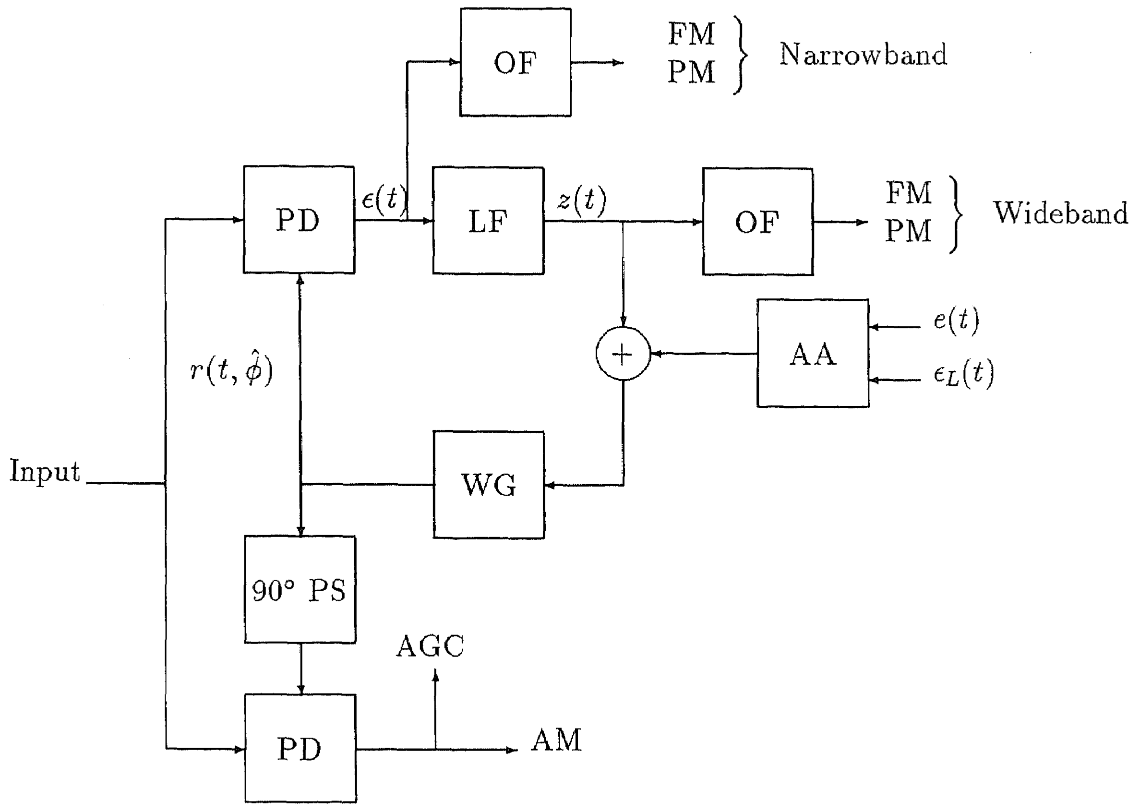

Figure 2.1: A General Model of PLLs

Most applications of a PLL can be considered as a special case of this general model. PLLs have many applications, but the following are the more generally used:

1. Carrier tracking
2. Suppressed carrier tracking
3. Coherent Demodulation of analog and digital signals
4. Symbol (Bit) synchronization
5. Frequency synthesis

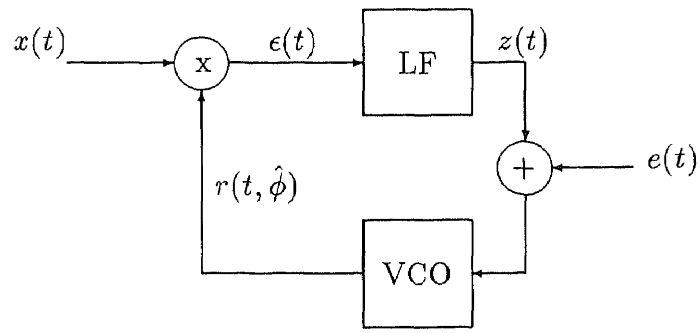

Figure 2.2: Carrier Tracking PLL

2.1 Carrier Tracking

Coherent communication is widely used at the present. Coherent demodulation basicaly means that the modulated signal is demodulated using a carrier that is a close replica of the input signal; exactly the same frequency and a small difference in phase. A PLL can reconstruct a carrier from that of the received signal, even if the signal is well below noise level. To achieve carrier tracking the loop operation is the same as that described in the introduction. Only an additive white gaussian noise may be present and an acquisition aid is added to help reduce the acquisition time. The block diagram of such a system is shown in figure 2.2. With the added noise,

$$x(t) = s(t, \phi) + n_i(t) \tag{2.1}$$

where

$$s(t, \phi) = \sqrt{2}A(t)\sin\phi(t) \tag{2.2}$$

and $n_i(t)$ is the background noise which is always considered white gaussian. $A(t)$ represents either analog or digital amplitude modulation, $\phi(t)$ is either an analog or a digital phase or frequency modulation. Also,

$$r(t, \hat{\phi}) = \sqrt{2}K_1 \cos \hat{\phi}(t)) \tag{2.3}$$

where $\hat{\phi}(t)$ is the loop estimate of $\phi(t)$. $e(t)$ in the diagram is the acquisition aid voltage. Here the waveform generator is a VCO and the phase detector is a simple multiplier. For the noise free case, the equations presented in the introduction are applicable here. The loop of figure 2 can be designed so that, even in the presence of noise, when the average of $\epsilon(t)$ is constant, the loop is phase locked and, therefore, is in the tracking mode. As soon as either $s(t, \phi)$ or $r(t, \hat{\phi})$ change phase, the output of the loop filter creates an error voltage proportional in magnitude and direction to the phase change. When both $z(t)$ and $e(t)$ are applied to the VCO, a change in frequency and phase in the VCO output follows so that it tracks the phase of the input signal. Therefore the loop retains lock, and stays in the tracking mode. This version of the PLL has found use in:

- Envelope detection
- PM and FM detection
- The synchronization of multiple clock frequencies in computers
- Multichannel receivers and transmitters
- The control of precision motor speed

2.2 Suppressed Carrier Tracking

For many different reasons, some communication schemes require a suppressed carrier transmission. Although $s(t, \phi)$ in such cases does not contain a carrier component, it is still possible, through a wide range of techniques using PLL to reconstruct the missing carrier component and then track it. Different approaches were suggested for suppressed carrier tracking; namely: Costas Loop, N^{th} power loop, data aided loops, decision directed loops, delay lock loops, hybrid loops, etc.

2.3 Coherent Demodulation of Analog Signals

Looking at the general model of a PLL one can see the different possibilities for demodulation of analog signals. Narrowband FM or PM can be extracted from the output of the phase detector of a the PLL, while wideband FM or PM demodulation can be retrieved from the loop filter's output.

AM coherent demodulation, on the other hand, is possible by using a coherent detector after phase shifting the VCO's output by 90°. In addition to AM detection this configuration can provide an Automatic Gain Control (AGC) or a lock indicator. It should be noted, however, that most phase detectors used in PLL applications are amplitude sensitive. Therefore, AGC is important where accurate control of loop parameters is required.

2.4 Coherent Demodulation of Digital Signals

Digital data is regularly used to modulate a subcarrier which in turn modulates the main carrier. If the subcarrier is phase modulated, the digital data can be recovered through another carrier tracking loop with a center frequency close to that of the subcarrier. The input to the second carrier tracking loop is taken from the output of the phase detector. Thus, the output of the second subcarrier tracking loop filter is the desired digital data. In the case when the information is modulated such that a suppressed carrier results as in PSK, a Costas loop should be used instead of the second carrier tracking loop. The output of the lower phase detector of Costas loop would be the baseband modulation signal. Digital AM signal demodulation is similar to that of analog AM signals.

2.5 Symbol (Bit) Synchronization Systems

In digital data communication it is vital to be able to achieve symbol synchronization in order to recover the data. Achieving symbol synchronization means determining the time when a modulation changes states. Although it is possible to use a separate channel to provide symbol synchronization information, it is more efficient to obtain this information directly from the received data signal. The block diagram in Figure 2.3 shows the model of a class of symbol synchronization systems as suggested by the maximum aposteriori estimation. The phase detector of such systems could have one of the following characteristics:

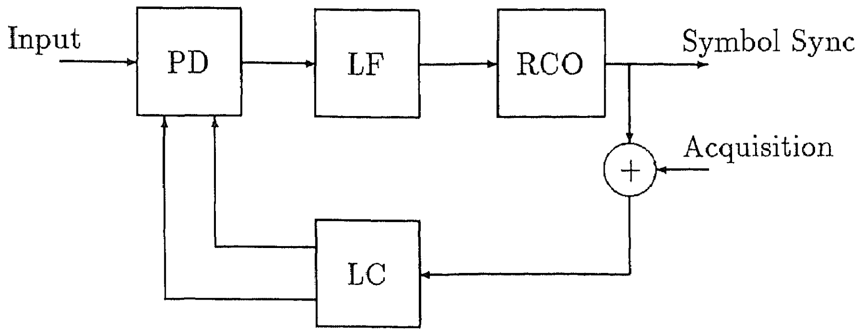

Figure 2.3: Block Diagram of Symbol (Bit) Synchronization System, RCO = Reference Controlled Oscillator, LC = Logic Circuit

- The Early-late gate
- Those which incorporate an absolute value approach
- A difference of squares approach
- The decision directed

The following are keys for Figure 2.3

- RCO = Reference Controlled Oscillator
- LC = Logic Circuit

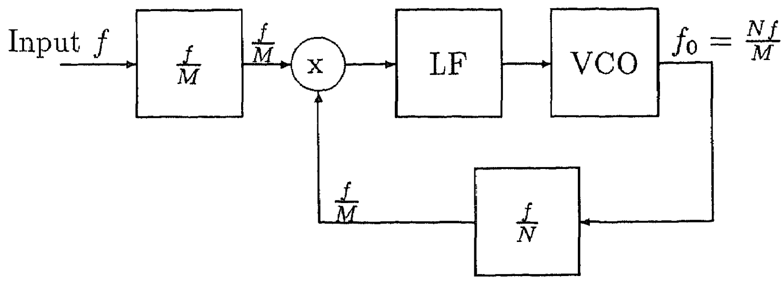

Figure 2.4: Frequency Division / Multiplication

2.6 Frequency Synthesis

Indirect frequency synthesizers of spectrally pure signals techniques rely heavily on the PLL. It is used in performing frequency division as well as multiplication (Fig. 2.4), and frequency translation (Fig. 2.5). These operations can be performed together to form a programmable frequency synthesizer. The divider/multiplier operation is very simple. Before entering the loop the signal is frequency divided by M and after the VCO the reference signal is again frequency divided by N, thus, the output of the VCO is the signal multiplied by N and divided by M in frequency. By the appropriate choice of M & N either division or multiplication can be performed. The loop for frequency translation is even simpler. Here the output of the VCO is mixed with a reference signal of frequency f_1. Thus the output of the VCO is shifted to a frequency $f_0 = f \pm f_1$.

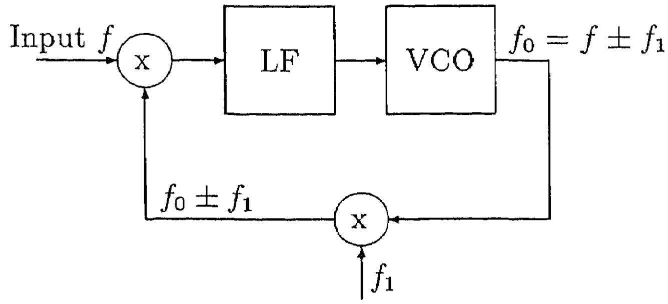

Figure 2.5: Frequency Translation

2.7 Operational Behavior of General PLL

As mentioned before, a PLL operation falls under two categories,

1. Acquisition mode
2. Synchronous or tracking mode

The performance of PLL could be statistical or deterministic depending on whether noise is present or not. In the rotating phasor form, and assuming that the amplitude is one,

$$s(t, \phi) = \mathrm{Real}[e^{j\phi(t)}] \tag{2.4}$$

$$r(t, \hat{\phi}) = \mathrm{Real}[e^{j\hat{\phi}(t)}] \tag{2.5}$$

the instantaneous angular velocities of the two phasors are,

$$\begin{aligned} \omega(t) &= \dot{\phi}(t) \text{ rad / sec} \\ \hat{\omega}(t) &= \dot{\hat{\phi}}(t) \text{ rad / sec} \end{aligned}$$

Even though the phase error $\Phi(t) = \phi(t) - \hat{\phi}(t)$ depends on the application and the mode of operation, the performance measures associated with the random process $\{\Phi(t)\}$ are essentially independent of the application.

2.7.1 Acquisition Mode

At time $t = t_0$ the two phasors in Eqs. 2.4 and 2.5, rotate at angular velocities of, $\dot{\phi}(t)|_{t=t_0} = \omega = \omega(t_0)$ and $\dot{\hat{\phi}}(t)|_{t=t_0} = \omega_0 = \hat{\omega}(t_0)$. Hence, at $t = t_0$ the relative velocity is given by

$$\Omega_0 = \dot{\Phi}(t_0) = \omega - \omega_0. \tag{2.6}$$

$\frac{\Omega_0}{2\pi}$ is known as the initial frequency detuning. The phase locked loop is said to have entered the synchronous mode if for $t = t_a$, $|\dot{\Phi}| < \epsilon_\Omega$ and $|\Phi(t) - 2n\pi| < \epsilon_\Phi$ for an integer n. Here, ϵ_Ω and ϵ_Φ represent the error of the derivative of the phase difference and the error of the phase difference respectively. The time $t_{acq} = t_a - t_0$ is the signal acquisition time. This value is sometimes referred to as either pull-in time or lock-in time.

In a noisy environment t_{acq} is a random variable with an N^{th} moment $T^n_{acq} = E[t^n_{acq}]$. This value depends on the initial state of the system. Sometimes the initial state itself is a random variable. If so, T^n_{acq} must be averaged over the initial state's probability density function (pdf).

After $t > t_a$,

$$\frac{\bar{\dot{\Phi}}(t)}{2\pi} = \frac{\omega(t) - \bar{\omega}_v(t)}{2\pi} \tag{2.7}$$

is called the mean residual frequency detuning. Here, $\bar{\omega}_v(t)$ is the average radian frequency of the synchronized wave generator and $\frac{\omega_0 - \bar{\omega}_v(t)}{2\pi}$ is the mean frequency shift.

If $\dot{\phi}(t) = \omega(t) =$ constant, then $\Omega_0 = \omega - \omega_0$ is also a constant. The largest value of Ω_0 $(= |\Omega_0|_m)$ from which the system can reach the synchronous state is known as either the pull-in range or lock-in range. Since the acquisition mode is nonlinear, only nonlinear methods can be used to model its behavior.

2.7.2 Synchronous Mode

As soon as $|\dot{\Phi}(t)| < \epsilon_\Omega$ and $|\Phi(t) - 2n\pi| < \epsilon_\Phi$, the loop is in the tracking mode, it tends to stay in it. In the presence of noise, and because of the instability of the wave generator, $\Phi(t)$ will fluctuate. Although linearized models have been developed to explain the behavior of PLLs, a number of performance measures are needed to explain the PLL's behavior. The most important of them is the time dependent conditional transition pdf $P(\Phi, t|\Phi_0, t_0)$[5] where ϕ is the phase error, Φ_0 is the initial condition on the phase and t_0 is the time at $t = 0$. Also, in some applications $P(\varphi(t), t|\varphi_0, t_0, n)$ is of interest as well as the steady state conditional transition pdf $P(\varphi|n)$, where $\varphi(t)$ is,

$$\varphi(t) = (\phi(t) + \pi) \mod (2\pi + [2n - 1]\pi) \tag{2.8}$$

Some applications require emphasis on the phase error $\Phi(t)$. In such cases, the application determines the requirements needed in $\Phi(t)$'s mean and average. Some cases restrict the mean to the order of few degrees, while others allow it to be as large as $45°$. If at some point in time Φ changes by $\pm 2\pi$, the process is called cycle-slipping. In relation to this phenomenon, the average rate of cycle-slipping $\bar{S}$

The time, T_{fp}, it takes for a sync failure to occur is a random variable whose statistical description through its pdf and moments are important. The first moment of this random variable is called the mean time to sync failure and it is noted by,

$$E(T_{fp}) = \tau(\frac{2\pi}{\Phi_0}) \tag{2.9}$$

This mean is very similar to the first passage time problem in the theory of Markov processes.

To complete the system performance characteristics, the probability of a sync failure $P(t)$ in the time interval $[t_0, t]$, as well as the probability of n cycle-slippings in the same interval of time, are of interest. Also the average time between cycle-slipping and the average time the system remains out of lock are important. The statistical properties of $\dot{\Phi}$ and $\bar{S}$ characterize the frequency stability of the synchronized generator.

2.8 Loop Equations in the Absence of Noise

In the following analysis of the PLL it will be assumed that the phase detector is a simple multiplier. Thus the loop block diagram is shown in figure 2.6. Also, it will be assumed that

$$s(t, \phi) = \sqrt{2}A(t) \sin \phi(t) \tag{2.10}$$

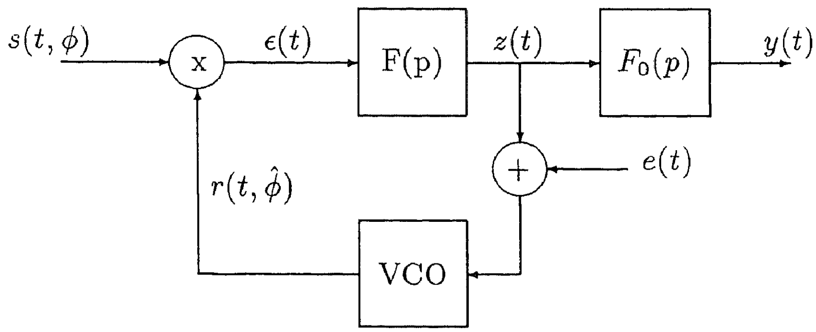

Figure 2.6: Carrier Tracking PLL

where $A(t)$ could be either a message that amplitude modulates the carrier, or caused by time varying multipath. It could also be a constant magnitude.

$$\phi(t) = \omega_0 t + \theta(t) \tag{2.11}$$

$\dfrac{\omega_0}{2\pi}$ is the center frequency of the input signal, and $\theta(t)$ is a message that is phase modulating the carrier. $\theta(t)$ could also be a constant phase. Let

$$r(t,\hat{\phi}) = \sqrt{2}K_1 \cos\hat{\phi}(t) \tag{2.12}$$

where

$$\hat{\phi}(t) = \omega_0 t + \hat{\theta}(t) \tag{2.13}$$

Ignoring the double frequency terms the output of the phase detector becomes,

$$\epsilon(t) = A(t)K_m K_1 \sin\Phi(t) \tag{2.14}$$

where K_m is the multiplier gain and

$$\Phi(t) = \phi(t) - \hat{\phi}(t) \tag{2.15}$$

and using equations (2.11) and (2.13),

$$\Phi(t) = \theta(t) - \hat{\theta}(t). \tag{2.16}$$

$\epsilon(t)$ is known as the dynamic phase error. At the output of the loop filter $z(t)$ is,

$$z(t) = F(p)\epsilon(t) \tag{2.17}$$

where $F(p)$ is known as the heaviside operator, and thus, z(t) is,

$$z(t) = \int_0^t f(t-\lambda)\epsilon(\lambda)d\lambda. \tag{2.18}$$

In order to derive the transfer function of the VCO, one should know that when the input of the VCO is zero then the oscillator operates at its natural frequency ω_0. It is assumed that the VCO change in frequency is linear with respect to the input voltage. Thus,

$$\frac{d\hat{\phi}(t)}{dt} = \omega_0 + K_v(z(t) + e(t)) \tag{2.19}$$

$$\hat{\phi}(t) = \omega_0 t + \int_0^t K_v(z(\lambda) + e(\lambda))d\lambda \tag{2.20}$$

By using equations (2.13) and (2.20), and writing in operator p notation,

$$\hat{\theta}(t) = \frac{K_v}{p}[z(t) + e(t)] \tag{2.21}$$

combining equations (2.21), (2.17), and (2.14) it follows that,

$$\hat{\theta}(t) = \frac{F(p)}{p}A(t)K_1K_vK_m \sin\Phi(t) + \frac{K_v}{p}e(t) \tag{2.22}$$

$$= \frac{KF(p)}{p}A(t)\sin\Phi(t) + \frac{K_v}{p}e(t) \tag{2.23}$$

which implies from equation (2.16),

$$\Phi(t) = \theta(t) - \frac{KF(p)}{p}[A(t)\sin\Phi(t)] - \frac{K_v}{p}e(t) \tag{2.24}$$

Since p denotes the derivative operation $\frac{d}{dt}$, equation (2.24) becomes,

$$\dot{\Phi}(t) = \dot{\theta}(t) - KF(p)[A(t)\sin\Phi(t)] - K_v e(t) \tag{2.25}$$

and replacing $F(p)$ by the convolution integral,

$$\frac{d\Phi(t)}{dt} = \frac{d\theta(t)}{dt} - K\int_0^t f(t-\lambda)A(\lambda)\sin\Phi(\lambda)d\lambda - K_v e(t) \tag{2.26}$$

Equation (2.26) is in the form of a nonlinear integro-differential equation. It represents the loop equation in the absence of noise. If $F(p)$ has n poles at the origin, the loop would be of the $(n+1)^{th}$ order.

2.9 Loop Equation in the Presence of Noise

Additive white noise is part of any electric system. In PLLs the fluctuation in the VCO and in the transmitter's local oscillator also have to be included as noise. Again assuming that,

$$\begin{aligned}
s(t,\phi) &= \sqrt{2}A(t)\sin\phi(t) \\
&= \sqrt{2}A(t)\sin(\omega_0 t + \theta(t)) \\
r(t,\hat{\phi}(t)) &= \sqrt{2}K_1\cos\hat{\phi}(t) \\
&= \sqrt{2}K_1\cos(w_0 t + \Theta(t))
\end{aligned}$$

where

$$\Theta(t) = \hat{\theta}(t) + \psi_2(t)$$

and $\psi_2(t)$ is the phase jitter noise produced by the VCO.

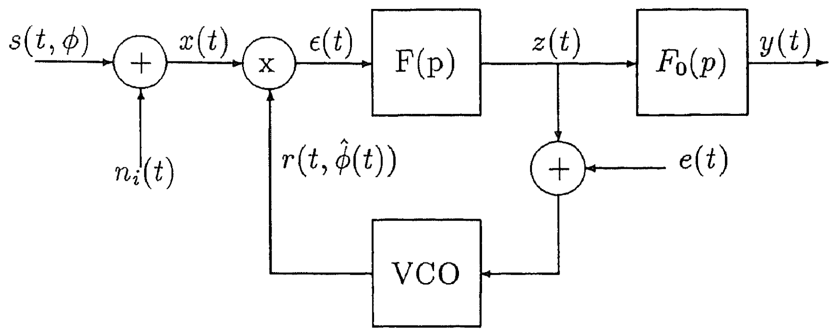

Figure 2.7: PLL in a Noisy Environment

It will be assumed that the additive noise $n_i(t)$ in figure 2.7 is a narrowband Gaussian random process (Appendix A), whose outocorrelation,

$$R_{n_i}(\tau) = \overline{N_i(\tau)N_i(t+\tau)} \tag{2.27}$$

From Appendix A,

$$R_{n_i}(\tau) = 2r(\tau)\cos\omega_0\tau. \tag{2.28}$$

The input to the PLL, $x(t)$, is the sum of the signal and noise,

$$\begin{aligned} x(t) &= s(t,\phi) + n_i(t) \\ &= \sqrt{2}[A(t)\sin\phi(t) + N_i(t)\cos\phi_i(t)]. \end{aligned}$$

Where,

$$\begin{aligned} \cos\phi_i(t) &= \cos(w_0 t + \theta_i(t)) \\ &= \cos(w_0 t + \theta(t) + \theta_i(t) - \theta(t)) \\ &= \cos(\phi(t) + \theta_i(t) - \theta(t)) \\ &= \cos\phi(t)\cos(\theta_i(t) - \theta(t)) - \sin\phi(t)\sin(\theta_i(t) - \theta(t)) \end{aligned}$$

Thus $x(t)$ becomes,

$$\begin{aligned} x(t) &= \sqrt{2}\,[A(t)\sin\phi(t) + N_i(t)\cos\phi(t)\cos(\theta_i(t)-\theta(t)) \\ &\quad - N_i(t)\sin\phi(t)\sin(\theta_i(t)-\theta(t))] \end{aligned} \tag{2.29}$$

Defining $N_c(t)$ and $N_s(t)$ as,

$$N_c(t) = N_i(t)\cos(\theta_i(t)-\theta(t)) \tag{2.30}$$

$$N_s(t) = N_i(t)\sin(\theta_i(t)-\theta(t)) \tag{2.31}$$

and,

$$N(t,\phi) = N_c(t)\cos\phi(t) - N_s(t)\sin\phi(t) \tag{2.32}$$

hence $x(t)$ becomes,

$$x(t) = \sqrt{2}\,[A(t)\sin\phi(t) - N_s(t)\sin\phi(t) + N_c(t)\cos\phi(t)] \tag{2.33}$$

$$= \sqrt{2}\,[A(t)\sin\phi(t) + N(t,\phi)] \tag{2.34}$$

Therefore, the ouput of the phase detector $\epsilon(t)$ is,

$$\epsilon(t) = K_1 K_m[A(t)\sin\Phi(t) + N(t,\Phi)] \tag{2.35}$$

and the output of the filter in the p operator notation is $z(t) = F(p)\epsilon(t)$, thus we get a VCO instantaneous frequency of,

$$\dot{\Theta}(t) = K_v(z(t) + e(t)) + \dot{\psi}_2(t) \tag{2.36}$$

Replacing $z(t)$ by its value in (2.17) the VCO phase output becomes,

$$\Theta(t) = \frac{K_v}{p}[F(p)\epsilon(t)] + \frac{K_v}{p}e(t) + \psi_2(t) \tag{2.37}$$

$$= \frac{KF(p)}{p}[A(t)\sin\Phi(t) + N(t,\Phi(t))] + \frac{K_v}{p}e(t) + \psi_2(t) \tag{2.38}$$

Since $\Phi(t) = \theta(t) - \Theta(t)$, we have,

$$\Phi(t) = \theta(t) - \frac{KF(p)}{p}[A(t)\sin\Phi(t) + N(t,\Phi(t))] + \frac{K_v}{p}e(t) + \psi_2(t) \tag{2.39}$$

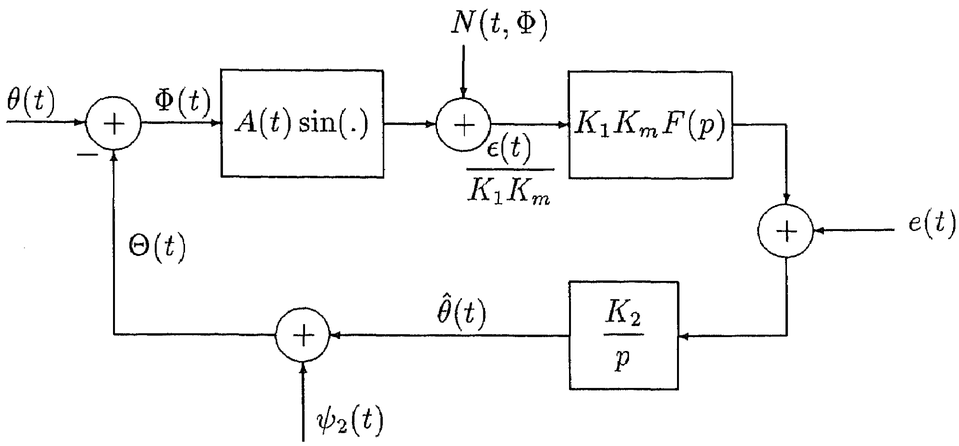

Figure 2.8: Mathematical Model of a PLL

Equation (2.39) is known as the loop equation. It should be noted that $\theta(t)$ includes three different processes,

$$\theta(t) = d(t) + M(t) + \psi_1(t) \tag{2.40}$$

where, $d(t)$ is the Doppler input, $M(t)$ is the digital or analog modulation, and $\psi_1(t)$ is the transmitter's oscillator phase instability process.

Equation (2.39) suggests a mathematical loop model depicted in Figure 2.8. This is a simple representation of the mathematical operations performed by a PLL on the phase. Looking at the first block, the input is $\Phi(t)$ and the output is $A(t)\sin\Phi(t)$ and then $N(t,\Phi(t))$ is added to form $\frac{\epsilon(t)}{K_1 K_m}$. The latter is then passed through a filter $F(p)$ with a gain $K_1 K_m$ to give the signal $z(t)$. Then $e(t)$ is added to form a voltage proportional to the instantaneous frequency. This voltage is passed through an integrator with a gain of K_v to obtain the phase estimate $\hat{\theta}(t)$.

The phase jitter is finally added to get $\Theta(t)$ which is in turn subtracted from the input phase to form the phase error $\Phi(t)$.

2.10 Linear Model of the Tracking Loop

In the tracking mode the phase error $\Phi(t)$ is small. Therefore, it is possible to approximate $\sin\Phi(t)$ by the phase error itself. Thus,

$$\Phi(t) = \theta(t) - K\frac{F(p)}{p}\left[A\Phi(t) + N_c(t)\right] - \psi_2(t) - \frac{K_v}{p}e(t) \tag{2.41}$$

where $N_c(t)$ is defined as in equation (2.30) and is assumed to be, $N_c(t) \gg N_s(t)\Phi(t)$. Replacing $\theta(t)$ in equation (2.41) by its value from equation (2.40), it follows,

$$\dot{\Phi}(t) = \dot{d}(t) + \dot{M}(t) - KF(p)\left[A\Phi(t) + N_c(t)\right] - K_v e(t) + \Delta\dot{\psi}(t) \tag{2.42}$$

where $\Delta\psi(t) = \psi_1(t) - \psi_2(t)$. This loop equation suggests the linear baseband equivalent loop model shown in Figure 2.9. The loop equation in (2.42) can be rearranged to get,

$$[p + AKF(p)]\,\dot{\Phi}(t) = p\left[d(t) + M(t) + \Delta\psi(t) - \frac{K_v}{p}e(t)\right] - KF(p)N_c(t) \tag{2.43}$$

$$\Phi(t) = \frac{p}{p + AKF(p)}\left[d(t) + M(t) + \Delta\psi - \frac{k_v}{p}e(t)\right] - \frac{AKF(p)}{p + AKF(p)}\frac{N_c(t)}{A} \tag{2.44}$$

Directly from figure 2.9 the closed loop transfer function is,

$$\begin{aligned} H_\Phi(p) &= \frac{\Theta(p)}{\theta(p)} && (2.45)\\ &= \frac{AKF(p)}{p + AKF(p)} && (2.46) \end{aligned}$$

It is possible to write $F(p)$ in terms of $H_\Phi(p)$,

$$F(p) = \frac{pH_\Phi(p)}{AK\left[1 - H_\Phi(p)\right]} \tag{2.47}$$

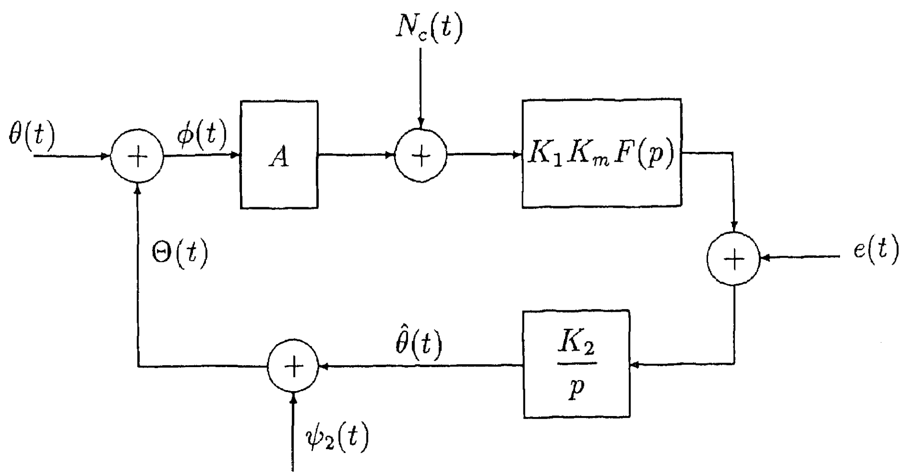

Figure 2.9: Linearized Model of a PLL

Since,

$$\frac{p}{p+AKF(p)} = \frac{p+AKF(p)-AKF(p)}{P+AKF(p)} \tag{2.48}$$

$$= \frac{p+AKF(p)}{p+AKF(p)} - \frac{AKF(p)}{p+AKF(p)} \tag{2.49}$$

$$= 1 - H_\Phi(p) \tag{2.50}$$

Thus equation (2.44) can be written as,

$$\Phi(t) = (1 - H_\Phi(p))\left[d(t) + M(t) + \Delta\psi - \frac{K_v}{p}e(t)\right] - H_\Phi(p)\frac{N_c(t)}{A} \tag{2.51}$$

Equation (2.51) can be separated into two components. Because the first part is multiplied by $1 - H_\Phi(p)$, it is the part rejected by the loop. The second component is multiplied by $H_\Phi(p)$. This is the part passed by the loop. Hence, the phase error is a result of two processes. First the noise normalized to the signal amplitude $\frac{N_c(t)}{A}$ is put through $H_\Phi(p)$. Second, $d(t) + M(t) + \Delta\psi(t) - \frac{K_v}{p}e(t)$ (the signal) is put through $1 - H_\Phi(p)$.

To summerize, we presented in this chapter some information regarding the nonlinear and linear theories of the PLL. These theories can help understand the tracking behavior of the PLL. In addition, some applications of PLLs were lso given. Next, in chapter 3 we will concentrate on the CCPLL through its mathematical model. All the material of this chapter can be found in greater detail in [4].

Chapter 3

N-Dimentional CCPLL (NCCPLL)

Following the introduction of the cross coupled PLL in chapter 1, this chapter will present the mathematical representation of the acquisition mode of the N cross coupled PLL (NCCPLL). Also, the loop equations will be developed. As it was mentioned earlier, NCCPLL is capable of seperating N FM or PM signals even if they are all at the same carrier frequency and they occupy the same frequency band. Also the relative powers of the signals has little effect. This chapter will follow the same format used in [6].

3.1 Acquisition Behavior of the NCCPLL

In this section the loop equations for the NCCPLL will be developed in the absence of noise. It is difficult to draw the full NCCPLL block diagram. Therefore, two graphs will be drawn, the first will consist of the N PLLs without the amplitude control, (see figure 3.1) while the second will include only the amplitude control. (see figure 3.2) Since the amplitude control is similar for each loop, only one set will be drawn.

3.1.1 Characteristic Equations

The input signal is assumed to be of the form:

$$S(t) = S_1(t) + S_2(t) + \cdots + S_N(t) \tag{3.1}$$

where $S_i(t)$ is an angle modulated signal, with a slowly varying amplitude,

$$S_i(t) = x_i(t)\sin\left(\omega_0 t + \psi_i(t)\right). \tag{3.2}$$

Let the amplitude control signals be denoted by,

$$\begin{aligned} y_{jRi}(t) &= \begin{cases} y_{jRi}(t) & i \neq j \\ 0 & i = j \end{cases} \\ y_{jIi}(t) &= \begin{cases} y_{jIi}(t) & i \neq j \\ 0 & i = j \end{cases} \end{aligned}$$

where the subscripts R and I stand for in-phase and quadrature components respectively. The indices, i and j, note the amplitude control from loop j to loop i. From figure 3.1 the output of the summer of loop i is:

$$V_i(t) = S(t) - \sum_{j=0}^{N}(W_{jRi} + W_{jIi}) \qquad i = 1, 2, \ldots, N$$

where from figure 3.2,

$$\begin{aligned} W_{jRi} &= y_{jRi}V_{Rj} \\ W_{jIi} &= y_{jIi}V_{Ij} \end{aligned}$$

the relation between y in the previous two equations and Y in figure 3.2 will be explained latter in this section. $V_i(t)$ becomes,

$$V_i(t) = S(t) - [y_i(t)] \bullet [U(t)] \tag{3.3}$$

where, A•B denotes the sum of the product of the rows of A by the columns of B.

$$y_i(t) = \begin{bmatrix} y_{1Ri}(t) & y_{1Ii}(t) \\ y_{2Ri}(t) & y_{2Ii}(t) \\ \vdots & \vdots \\ y_{NRi}(t) & y_{NIi}(t) \end{bmatrix} \tag{3.4}$$

$$U(t) = \begin{bmatrix} V_{R1}(t) & V_{R2}(t) & \cdots & V_{RN}(t) \\ V_{I1}(t) & V_{I2}(t) & \cdots & V_{IN}(t) \end{bmatrix} \tag{3.5}$$

Assuming that the output of the VCO of loop i is an estimate of the input signal $S_i(t)$ we have,

$$V_{oi}(t) = B_i \cos(\omega_0 t + K_{vi}\phi_i(t)) \tag{3.6}$$

Then from figure (3.2),

$$V_{Ri}(t) = B_i \sin(\omega_0 t + K_{vi}\phi_i(t))$$
$$V_{Ii}(t) = B_i \cos(\omega_0 t + K_{vi}\phi_i(t))$$

Clearly, from equation (3.6) the input to the VCO or the output of the loop filter at loop i is $\dot{\phi}_i(t)$. Assuming that the loop filter is low-pass we have from figure 3.1:

$$\begin{aligned} \dot{\phi}_i(t) &= V_{oi}(t)V_i(t) * h_i(t) \\ &= \{V_{oi}(t)S(t) - V_{oi}(t)[y_i(t)] \bullet [U(t)] * h_i(t) \end{aligned}$$

Using the following sinusoidal identities,

$$\sin(a)\cos(b) = \frac{1}{2}[\sin(a-b) + \sin(a+b)]$$
$$\cos(a)\cos(b) = \frac{1}{2}[\cos(a-b) + \cos(a+b)]$$

and neglecting double frequency terms, we get:

$$
\begin{aligned}
\dot{\phi}_i(t) &= \frac{B_i}{2}\{[x_1(t)\sin(\psi_1(t) - K_{vi}\phi_i(t)) + x_2(t)\sin(\psi_2(t) - K_{vi}\phi_i(t)) \\
&\quad + \cdots + x_N(t)\sin(\psi_N(t) - K_{vi}\phi_i(t))] - \begin{bmatrix} y_{1Ri} & y_{1Ii} \\ y_{2Ri} & y_{2Ii} \\ \vdots & \vdots \\ y_{NRi} & y_{NIi} \end{bmatrix} \bullet \\
&\quad \left[\begin{matrix} B_1\sin(K_{v1}\phi_1(t) - K_{vi}\phi_i(t)) & B_2\sin(K_{v2}\phi_2(t) - K_{vi}\phi_i(t)) \\ B_1\cos(K_{v1}\phi_1(t) - K_{vi}\phi_i(t)) & B_2\cos(K_{v2}\phi_2(t) - K_{vi}\phi_i(t)) \end{matrix}\right. \\
&\quad \left.\begin{matrix} \cdots & B_N\sin(K_{vN}\phi_N(t) - K_{vi}\phi_i(t)) \\ \cdots & B_N\cos(K_{vN}\phi_N(t) - K_{vi}\phi_i(t)) \end{matrix}\right]\} * h_i(t)
\end{aligned}
\tag{3.7}
$$

Making the following variable changes, (ω_n is the PLLs natural frequency)

$$
\begin{aligned}
\Phi_i(t) &= K_{vi}\phi_i(t) && (3.8) \\
t &= \tau\omega_n \\
\Longrightarrow dt &= \omega_n d\tau \\
\Longrightarrow \frac{d\Phi(t)}{dt} &= K_v\frac{d\phi(\tau)}{\omega_n d\tau} && (3.9) \\
Y_{ji} &= y_{ji}\frac{A}{B_i} && (3.10)
\end{aligned}
$$

it follows,

$$
\begin{aligned}
\dot{\Phi}_i(t) &= \frac{B_iK_{vi}}{2\omega_n}\{[x_1(t)\sin(\psi_1(t) - \Phi_i(t)) + x_2(t)\sin(\psi_2(t) - \Phi_i(t)) \\
&\quad + \cdots + x_N(t)\sin(\psi_N(t) - \Phi_i(t))] - A\begin{bmatrix} Y_{1Ri} & Y_{1Ii} \\ Y_{2Ri} & Y_{2Ii} \\ \vdots & \vdots \\ Y_{NRi} & Y_{NIi} \end{bmatrix} \bullet \\
&\quad \left[\begin{matrix} \sin(\Phi_1(t) - \Phi_i(t)) & \sin(\Phi_2(t) - \Phi_i(t)) \\ \cos(\Phi_1(t) - \Phi_i(t)) & \cos(\Phi_2(t) - \Phi_i(t)) \end{matrix}\right. \\
&\quad \left.\begin{matrix} \cdots & \sin(\Phi_N(t) - \Phi_i(t)) \\ \cdots & \cos(\Phi_N(t) - \Phi_i(t)) \end{matrix}\right]\} * h_i(t)
\end{aligned}
\tag{3.11}
$$

Defining the following,

$$
\alpha_i \triangleq \frac{B_iK_{vi}A}{2\omega_n} \tag{3.12}
$$

equation (3.11) becomes,

$$
\begin{aligned}
\dot{\Phi}_i(t) &= \alpha_i \left\{ \left[\frac{x_1(t)}{A} \sin\left(\psi_1(t) - \Phi_i(t)\right) + \frac{x_2(t)}{A} \sin\left(\psi_2(t) - \Phi_i(t)\right) \right.\right. \\
&\quad \left. + \cdots + \frac{x_N(t)}{A} \sin\left(\psi_N(t) - \Phi_i(t)\right) \right] - \begin{bmatrix} Y_{1Ri} & Y_{1Ii} \\ Y_{2Ri} & Y_{2Ii} \\ \vdots & \vdots \\ Y_{NRi} & Y_{NIi} \end{bmatrix} \bullet \\
&\quad \begin{bmatrix} \sin\left(\Phi_1(t) - \Phi_i(t)\right) & \sin\left(\Phi_2(t) - \Phi_i(t)\right) \\ \cos\left(\Phi_1(t) - \Phi_i(t)\right) & \cos\left(\Phi_2(t) - \Phi_i(t)\right) \end{bmatrix} \\
&\quad \left. \begin{matrix} \cdots & \sin\left(\Phi_N(t) - \Phi_i(t)\right) \\ \cdots & \cos\left(\Phi_N(t) - \Phi_i(t)\right) \end{matrix} \right]\right\} * h_i(t) \qquad (3.13)
\end{aligned}
$$

Equation (3.11) can be written as,

$$
\dot{\Phi}_i(t) = \alpha_i \left[\phi_{1i}(t) + \phi_{2i}(t) + \cdots + \phi_{Ni}(t)\right] * h_i(t) \qquad (3.14)
$$

where

$$
\begin{aligned}
\phi_{ji} &= [\frac{x_j(t)}{A} \sin(\psi_j(t) - \Phi_i(t)) - Y_{jRi}(t) \sin(\Phi_j(t) - \Phi_i(t)) \\
&\quad - Y_{jIi}(t) \cos(\Phi_j(t) - \Phi_i(t))]. \qquad (3.15)
\end{aligned}
$$

In most cases it is more appropriate to write equation (3.11) in dot product form as follows,

$$
\begin{aligned}
\dot{\Phi}_i(t) &= \alpha_i \begin{bmatrix} \frac{x_1(t)}{A} & \frac{x_2(t)}{A} & \cdots & \frac{x_i(t)}{A} & \cdots & \frac{x_N(t)}{A} \\ Y_{1Ri} & Y_{2Ri} & \cdots & 0 & \cdots & Y_{NRi} \\ Y_{1Ii} & Y_{2Ii} & \cdots & 0 & \cdots & Y_{NIi} \end{bmatrix} \bullet \\
&\quad \begin{bmatrix} \sin(\psi_1(t) - \Phi_i(t)) & \sin(\Phi_1(t) - \Phi_i(t)) \\ \sin(\psi_2(t) - \Phi_i(t)) & \sin(\Phi_2(t) - \Phi_i(t)) \\ \vdots & \vdots \\ \sin(\psi_i(t) - \Phi_i(t)) & 0 \\ \vdots & \vdots \\ \sin(\psi_N(t) - \Phi_i(t)) & \sin(\Phi_N(t) - \Phi_i(t)) \end{bmatrix}
\end{aligned}
$$

$$
\left.\begin{matrix} \cos(\Phi_1(t) - \Phi_i(t)) \\ \cos(\Phi_2(t) - \Phi_i(t)) \\ \vdots \\ 1 \\ \vdots \\ \cos(\Phi_N(t) - \Phi_i(t)) \end{matrix}\right] * h_i(t) \tag{3.16}
$$

3.1.2 Amplitude Control Equations

Equation (3.13) or (3.14) are differential equations that depend on the amplitude control signals $Y_{jRi}(t)$ and $Y_{jIi}(t)$. These signals can be found from figure (3.2) as follows: first let us evaluate the input to the integrator, $V_{jRi}(t)$ and $V_{jIi}(t)$,

$$
\begin{aligned}
V_{jRi}(t) &= V_{Rj}(t)V_i(t) \\
&= \frac{B_j}{2}\{[x_1(t)\cos(\psi_1(t) - K_{vj}\phi_j(t)) + x_2(t)\cos(\psi_2(t) - K_{vj}\phi_j(t)) \\
&\quad + \cdots + x_N(t)\cos(\psi_N(t) - K_{vj}\phi_j(t))] - \begin{bmatrix} y_{1Ri} & y_{1Ii} \\ y_{2Rj} & y_{2Ii} \\ \vdots & \vdots \\ y_{NRi} & y_{NIi} \end{bmatrix} \bullet \\
&\quad \left[\begin{matrix} B_1\cos(K_{v1}\phi_1(t) - K_{vj}\phi_j(t)) & B_2\cos(K_{v2}\phi_2(t) - K_{vj}\phi_j(t)) \\ B_1\sin(K_{v1}\phi_1(t) - K_{vj}\phi_j(t)) & B_2\sin(K_{v2}\phi_2(t) - K_{vj}\phi_j(t)) \end{matrix}\right. \\
&\quad \left.\begin{matrix} \cdots & B_N\cos(K_{vN}\phi_N(t) - K_{vj}\phi_j(t)) \\ \cdots & B_N\sin(K_{vN}\phi_N(t) - K_{vj}\phi_j(t)) \end{matrix}\right]\}
\end{aligned} \tag{3.17}
$$

Also from figure (3.2) it is evident that,

$$
\begin{aligned}
\dot{y}_{jRi}(t) &= K_{jRi}V_{jRi} * G_{jRi} \\
&= \frac{B_jK_{jRi}}{2}\{[x_1(t)\cos(\psi_1(t) - K_{vj}\phi_j(t)) + x_2(t)\cos(\psi_2(t) - K_{vj}\phi_j(t)) \\
&\quad + \cdots + x_N(t)\cos(\psi_N(t) - K_{vj}\phi_j(t))] - \begin{bmatrix} y_{1Ri} & y_{1Ii} \\ y_{2Rj} & y_{2Ii} \\ \vdots & \vdots \\ y_{NRi} & y_{NIi} \end{bmatrix} \bullet
\end{aligned}
$$

$$\left[\begin{array}{ll} B_1\cos\left(K_{v1}\phi_1(t)-K_{vj}\phi_j(t)\right) & B_2\cos\left(K_{v2}\phi_2(t)-K_{vj}\phi_j(t)\right) \\ B_1\sin\left(K_{v1}\phi_1(t)-K_{vj}\phi_j(t)\right) & B_2\sin\left(K_{v2}\phi_2(t)-K_{vj}\phi_j(t)\right) \end{array}\right.$$

$$\left.\begin{array}{ll} \cdots & B_N\cos\left(K_{vN}\phi_N(t)-K_{vj}\phi_j(t)\right) \\ \cdots & B_N\sin\left(K_{vN}\phi_N(t)-K_{vj}\phi_j(t)\right) \end{array}\right]\Bigg\} * G_{jRi} \tag{3.18}$$

Making the same variable changes as in equations (3.8), (3.9) and (3.10), we get,

$$\begin{aligned} \dot{Y}_{jRi}(t) \quad = \quad & \frac{B_jK_{jRi}}{2\omega_n}\left\{\left[x_1(t)\cos\left(\psi_1(t)-\Phi_j(t)\right)+x_2(t)\cos\left(\psi_2(t)-\Phi_j(t)\right)\right.\right. \\ & \left.+\cdots+x_N(t)\cos\left(\psi_N(t)-\Phi_j(t)\right)\right]-\left[\begin{array}{cc} Y_{1Ri} & Y_{1Ii} \\ Y_{2Rj} & Y_{2Ii} \\ \vdots & \vdots \\ Y_{NRi} & Y_{NIi} \end{array}\right]\bullet \\ & \left[\begin{array}{ll} \cos\left(\Phi_1(t)-\Phi_j(t)\right) & \cos\left(\Phi_2(t)-\Phi_j(t)\right) \\ \sin\left(\Phi_1(t)-\Phi_j(t)\right) & \sin\left(\Phi_2(t)-\Phi_j(t)\right) \end{array}\right. \\ & \left.\left.\begin{array}{ll} \cdots & \cos\left(\Phi_N(t)-\Phi_j(t)\right) \\ \cdots & \sin\left(\Phi_N(t)-\Phi_j(t)\right) \end{array}\right]\right\} * G_{jRi} \end{aligned} \tag{3.19}$$

Also defining the following,

$$\beta_j \triangleq \frac{AB_jK_{ji}}{2\omega_n} \tag{3.20}$$

where it is assumed that $K_{jRi} = K_{jIi} = K_{ji}$. Thus,

$$\begin{aligned} \dot{Y}_{jRi}(t) \quad = \quad & \beta_j\left\{\left[x_1(t)\cos\left(\psi_1(t)-\Phi_j(t)\right)+x_2(t)\cos\left(\psi_2(t)-\Phi_j(t)\right)\right.\right. \\ & \left.+\cdots+x_N(t)\cos\left(\psi_N(t)-\Phi_j(t)\right)\right]-\left[\begin{array}{cc} Y_{1Ri} & Y_{1Ii} \\ Y_{2Rj} & Y_{2Ii} \\ \vdots & \vdots \\ Y_{jRi} & Y_{jIi} \\ \vdots & \vdots \\ Y_{NRi} & Y_{NIi} \end{array}\right]\bullet \\ & \left[\begin{array}{lll} \cos\left(\Phi_1(t)-\Phi_j(t)\right) & \cos\left(\Phi_2(t)-\Phi_j(t)\right) & \cdots \\ \sin\left(\Phi_1(t)-\Phi_j(t)\right) & \sin\left(\Phi_2(t)-\Phi_j(t)\right) & \cdots \end{array}\right. \\ & \left.\left.\begin{array}{lll} 1 & \cdots & \cos\left(\Phi_N(t)-\Phi_j(t)\right) \\ 0 & \cdots & \sin\left(\Phi_N(t)-\Phi_j(t)\right) \end{array}\right]\right\} * G_{jRi} \end{aligned} \tag{3.21}$$

The solution of this differential equation takes the form,

$$Y_{jRi}(t) \quad = \quad \left\{\left[x_1(t)\cos\left(\psi_1(t)-\Phi_j(t)\right)+x_2(t)\cos\left(\psi_2(t)-\Phi_j(t)\right)\right.\right.$$

$$
+\cdots+x_N(t)\cos(\psi_N(t)-\Phi_j(t))]-\begin{bmatrix} Y_{1Ri} & Y_{1Ii} \\ Y_{2Rj} & Y_{2Ii} \\ \vdots & \vdots \\ Y_{jRi} & Y_{jIi} \\ \vdots & \vdots \\ Y_{NRi} & Y_{NIi} \end{bmatrix} \bullet
$$

$$
\begin{bmatrix} \cos(\Phi_1(t)-\Phi_j(t)) & \cos(\Phi_2(t)-\Phi_j(t)) & \cdots \\ \sin(\Phi_1(t)-\Phi_j(t)) & \sin(\Phi_2(t)-\Phi_j(t)) & \cdots \end{bmatrix}
$$

$$
\left.\begin{matrix} 0 & \cdots & \cos(\Phi_N(t)-\Phi_j(t)) \\ 0 & \cdots & \sin(\Phi_N(t)-\Phi_j(t)) \end{matrix}\right]\Bigg\} * F_{jRi} \tag{3.22}
$$

where

$$
F_{jRi}(t)=\mathcal{L}^{-1}\left[\frac{\beta_j G_{jRi}(s)}{s+\beta_j G_{jRi}(s)}\right]
$$

and

$$
G_{jRi}(s)=\mathcal{L}\left[G_{jRi}(t)\right].
$$

Similarly, for the imaginary part we have,

$$
\begin{aligned}
Y_{jIi}(t) \quad = \quad & \left\{\left[\frac{x_1(t)}{A}\sin(\psi_1(t)-\Phi_j(t))+\frac{x_2(t)}{A}\sin(\psi_2(t)-\Phi_j(t))\right.\right. \\
& \left.+\cdots+\frac{x_N(t)}{A}\sin(\psi_N(t)-\Phi_j(t))\right]-\begin{bmatrix} Y_{1Ri} & Y_{1Ii} \\ Y_{2Ri} & Y_{2Ii} \\ \vdots & \vdots \\ Y_{jRi} & Y_{jIi} \\ \vdots & \vdots \\ Y_{NRi} & Y_{NIi} \end{bmatrix} \bullet
\end{aligned}
$$

$$
\begin{bmatrix} \sin(\Phi_1(t)-\Phi_j(t)) & \sin(\Phi_2(t)-\Phi_j(t)) & \cdots \\ \cos(\Phi_1(t)-\Phi_j(t)) & \cos(\Phi_2(t)-\Phi_j(t)) & \cdots \end{bmatrix}
$$

$$
\left.\left.\begin{matrix} 0 & \cdots & \sin(\Phi_N(t)-\Phi_j(t)) \\ 0 & \cdots & \cos(\Phi_N(t)-\Phi_j(t)) \end{matrix}\right]\right\} * F_{jRi} \tag{3.23}
$$

where

$$
F_{jIi}(t)=\mathcal{L}^{-1}\left[\frac{\beta_j G_{jIi}(s)}{s+\beta_j G_{jIi}(s)}\right]
$$

and

$$
G_{jIi}(s)=\mathcal{L}\left[G_{jIi}(t)\right].
$$

Equations (3.22) and (3.23) can also be written in their respective dot product notations,

$$
\begin{aligned}
Y_{jRi} \;=\; & \begin{bmatrix} \frac{x_1(t)}{A} & \frac{x_2(t)}{A} & \cdots & \frac{x_i(t)}{A} & \cdots & \frac{x_j(t)}{A} & \cdots & \frac{x_N(t)}{A} \\ Y_{1Ri} & Y_{2Ri} & \cdots & 0 & \cdots & Y_{jRi} & \cdots & Y_{NRi} \\ Y_{1Ii} & Y_{2Ii} & \cdots & 0 & \cdots & Y_{jIi} & \cdots & Y_{NIi} \end{bmatrix} \bullet \\
& \begin{bmatrix} \cos(\psi_1(t)-\Phi_j(t)) & \cos(\Phi_1(t)-\Phi_j(t)) & \sin(\Phi_1(t)-\Phi_j(t)) \\ \cos(\psi_2(t)-\Phi_j(t)) & \cos(\Phi_2(t)-\Phi_j(t)) & \sin(\Phi_2(t)-\Phi_j(t)) \\ \vdots & \vdots & \vdots \\ \cos(\psi_i(t)-\Phi_j(t)) & \cos(\Phi_i(t)-\Phi_j(t)) & \sin(\Phi_i(t)-\Phi_j(t)) \\ \vdots & \vdots & \vdots \\ \cos(\psi_j(t)-\Phi_j(t)) & 0 & 0 \\ \vdots & \vdots & \vdots \\ \cos(\psi_N(t)-\Phi_j(t)) & \cos(\Phi_N(t)-\Phi_j(t)) & \sin(\Phi_N(t)-\Phi_j(t)) \end{bmatrix} * F_{jRi}(t)
\end{aligned} \tag{3.24}
$$

$$
\begin{aligned}
Y_{jIi} \;=\; & \begin{bmatrix} \frac{x_1(t)}{A} & \frac{x_2(t)}{A} & \cdots & \frac{x_i(t)}{A} & \cdots & \frac{x_j(t)}{A} & \cdots & \frac{x_N(t)}{A} \\ Y_{1Ri} & Y_{2Ri} & \cdots & 0 & \cdots & Y_{jRi} & \cdots & Y_{NRi} \\ Y_{1Ii} & Y_{2Ii} & \cdots & 0 & \cdots & Y_{jIi} & \cdots & Y_{NIi} \end{bmatrix} \bullet \\
& \begin{bmatrix} \sin(\psi_1(t)-\Phi_j(t)) & \sin(\Phi_1(t)-\Phi_j(t)) \\ \sin(\psi_2(t)-\Phi_j(t)) & \sin(\Phi_2(t)-\Phi_j(t)) \\ \vdots & \vdots \\ \sin(\psi_i(t)-\Phi_j(t)) & \sin(\Phi_i(t)-\Phi_j(t)) \\ \vdots & \vdots \\ \sin(\psi_j(t)-\Phi_j(t)) & 0 \\ \vdots & \vdots \\ \sin(\psi_N(t)-\Phi_j(t)) & \sin(\Phi_N(t)-\Phi_j(t)) \end{bmatrix}
\end{aligned}
$$

$$\begin{bmatrix} \cos(\Phi_1(t) - \Phi_j(t)) \\ \cos(\Phi_2(t) - \Phi_j(t)) \\ \vdots \\ \cos(\Phi_i(t) - \Phi_j(t)) \\ \cdots \\ 0 \\ \vdots \\ \cos(\Phi_N(t) - \Phi_J(t)) \end{bmatrix} * F_{jIi}(t) \tag{3.25}$$

Because Y_{jRi} and Y_{jIi} on the right hand side of equations (3.24) and (3.25) are each multiplied by a zero term, they are removed from the equations. Hence, Y_{jRi} and Y_{jIi} depend on other signals and control parameters only. If $F_{jRi}(t) = F_{jIi}(t) = F_{ji} = F_{ki} = F_j$; low pass responce, and assuming that the system is in tracking mode, that is

$$\Phi_j(t) = \hat{\psi}_j(t) \tag{3.26}$$

$$\tag{3.27}$$

then,

$$\frac{x_j(t)}{A} \cos\left(\psi_j(t) - \hat{\psi}_j(t)\right) * F_j(t) = \frac{x_j(t)}{A} \cos\left(\psi_j(t) - \hat{\psi}_j(t)\right) \tag{3.28}$$

$$\frac{x_j(t)}{A} \cos\left(\psi_j(t) - \hat{\psi}_i(t)\right) * F_j(t) = \frac{x_j(t)}{A} \delta_{ji} \cos\left(\psi_j(t) - \hat{\psi}_i(t) + \lambda_{ji}\right) \tag{3.29}$$

where δ_{ji} and λ_{ji} are the damping factor and the phase shift introduced by the filter $F_j(t)$. Equations (3.22) and (3.23) can be written as,

$$Y_{jRi}(t) = \frac{x_j(t)}{A} \cos\left(\psi_j(t) - \hat{\psi}_j(t)\right) + E_{jRi}(t) \tag{3.30}$$

$$Y_{jIi}(t) = \frac{x_j(t)}{A} \sin\left(\psi_j(t) - \hat{\psi}_j(t)\right) + E_{jIi}(t) \tag{3.31}$$

Where the error terms,

$$E_{jRi}(t) = \sum_{\substack{k=1 \\ k \neq j}}^{N} \left[\frac{x_k(t)}{A} \delta_{ik} \cos\left(\psi_k(t) - \hat{\psi}_j(t) + \lambda_{ik}\right) \right.$$

$$-\delta_{jk}\left[Y_{kRi}\cos\left(\hat{\psi}_k(t)-\hat{\psi}_j(t)\right)+Y_{kIi}\sin\left(\hat{\psi}_k(t)-\hat{\psi}_j(t)+\lambda_{jk}\right)\right] \quad (3.32)$$

$$E_{jIi}(t) = \sum_{\substack{k=1\\k\neq j}}^{N}\left[\frac{x_k(t)}{A}\delta_{ik}\sin\left(\psi_k(t)-\hat{\psi}_j(t)+\lambda_{ik}\right)\right.$$
$$\left.-\delta_{jk}\left[Y_{kRi}\sin\left(\hat{\psi}_k(t)-\hat{\psi}_j(t)\right)+Y_{kIi}\cos\left(\hat{\psi}_k(t)-\hat{\psi}_j(t)+\lambda_{jk}\right)\right]\right] \quad (3.33)$$

Equations (3.29) and (3.30) can be rearranged to get,

$$\begin{aligned}\frac{x_j(t)}{A}\cos\left(\psi_j(t)-\hat{\psi}_j(t)\right) &= Y_{jRi}(t)-E_{jRi}(t)\\ \frac{x_j(t)}{A}\sin\left(\psi_j(t)-\hat{\psi}_j(t)\right) &= Y_{jIi}(t)-E_{jIi}(t)\end{aligned}$$

Squaring both sides of each equation and then adding, we get,

$$\frac{x_j^2(t)}{A^2}=\left[Y_{jRi}(t)-E_{jRi}(t)\right]^2+\left[Y_{jIi}(t)-E_{jIi}(t)\right]^2 \quad (3.34)$$

Thus, the instantaneous amplitude estimate of each signal can be found by:

$$x_j(t)=A\sqrt{\left[Y_{jRi}(t)-E_{jRi}(t)\right]^2+\left[Y_{jIi}(t)-E_{jIi}(t)\right]^2} \quad (3.35)$$

If the damping factor of each filter is small enough the error terms can be neglected and the amplitude estimates become,

$$x_i(t)=A\sqrt{Y_{jRi}^2(t)+Y_{jIi}^2(t)} \quad (3.36)$$

Hence, from equation (3.15) we have

$$\phi_{ji}=0 \qquad \text{for} \quad j\neq i$$

and thus, from (3.14) and (3.15), since $Y_{jRj}=Y_{jIj}=0$ we have,

$$\begin{aligned}\dot{\Phi}_i(t) &= \phi_{ii}(t)\\ &= \frac{\alpha_i}{A}x_i(t)\sin\left(\psi_i(t)-\hat{\psi}_i(t)\right)*h_i(t) \quad (3.37)\\ &= \frac{B_iK_{vi}}{2\omega_n}x_i(t)\sin\left(\psi_i(t)-\hat{\psi}_i(t)\right)*h_i(t) \quad (3.38)\end{aligned}$$

Since $\dot{\Phi}_i(t)=\dot{\hat{\psi}}_i(t)$ it is the derivative of the phase estimate. Thus, if the estimate is good, FM or PM is acheived.

3.2 2CCPLL

In [7], the differential equations for two CCPLLs were developed. As a test, let us develop these expressions from equation (3.14). With $N = 2$ we get,

$$\begin{aligned}
\dot{\Phi}_1(t) &= \alpha_1 \left[\phi_{11}(t) + \phi_{21}(t)\right] \\
&= \alpha_1[\frac{x_1(t)}{A} \sin\left(\psi_1(t) - \Phi_1(t)\right) + \frac{x_2(t)}{A} \sin\left(\psi_2(t) - \Phi_1(t)\right) \\
&\quad - Y_{2R1} \sin\left(\Phi_2(t) - \Phi_1(t)\right) - Y_{2I1} \cos\left(\Phi_2(t) - \Phi_1(t)\right)] * h_1(t) \qquad (3.39) \\
\dot{\Phi}_2(t) &= \alpha_2 \left[\phi_{22}(t) + \phi_{12}(t)\right] \\
&= \alpha_2[\frac{x_1(t)}{A} \sin\left(\psi_1(t) - \Phi_2(t)\right) + \frac{x_2(t)}{A} \sin\left(\psi_2(t) - \Phi_2(t)\right) \\
&\quad - Y_{1R2} \sin\left(\Phi_1(t) - \Phi_2(t)\right) - Y_{1I2} \cos\left(\Phi_1(t) - \Phi_2(t)\right)] * h_2(t) \qquad (3.40)
\end{aligned}$$

The amplitude control equations can be found by evaluating equations (3.22) and (3.23),

$$\begin{aligned}
Y_{1R2} &= \left[\frac{x_1(t)}{A} \sin\left(\psi_1(t) - \Phi_1(t)\right) + \frac{x_2(t)}{A} \sin\left(\psi_2(t) - \Phi_1(t)\right)\right] * F_{1R2} \qquad (3.41) \\
Y_{1I2} &= \left[\frac{x_1(t)}{A} \cos\left(\psi_1(t) - \Phi_1(t)\right) + \frac{x_2(t)}{A} \cos\left(\psi_2(t) - \Phi_1(t)\right)\right] * F_{1I2} \qquad (3.42) \\
Y_{2R1} &= \left[\frac{x_1(t)}{A} \sin\left(\psi_1(t) - \Phi_2(t)\right) + \frac{x_2(t)}{A} \sin\left(\psi_2(t) - \Phi_2(t)\right)\right] * F_{2R1} \qquad (3.43) \\
Y_{2I1} &= \left[\frac{x_1(t)}{A} \cos\left(\psi_1(t) - \Phi_2(t)\right) + \frac{x_2(t)}{A} \cos\left(\psi_2(t) - \Phi_2(t)\right)\right] * F_{2I1} \qquad (3.44)
\end{aligned}$$

Also from equations (3.35), (3.43) and (3.44), we find,

$$\begin{aligned}
\dot{\Phi}_1(t) &= \frac{\alpha_1}{A} x_1(t) \sin\left(\psi_1(t) - \Phi_1(t)\right) * h_1(t) \qquad (3.45) \\
\dot{\Phi}_2(t) &= \frac{\alpha_2}{A} x_2(t) \sin\left(\psi_2(t) - \Phi_2(t)\right) * h_2(t) \qquad (3.46)
\end{aligned}$$

These equations are identical to those found in [7].

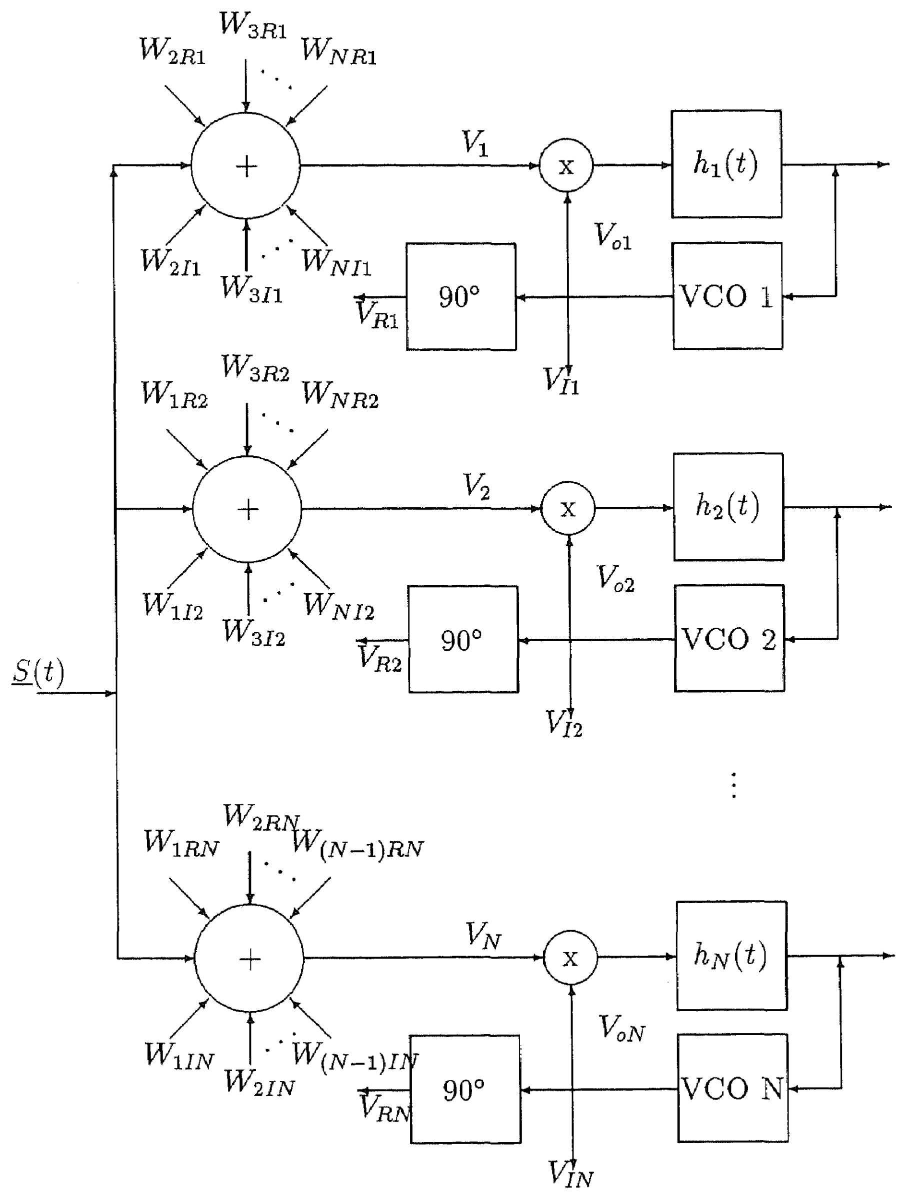

Figure 3.1: NCCPLL

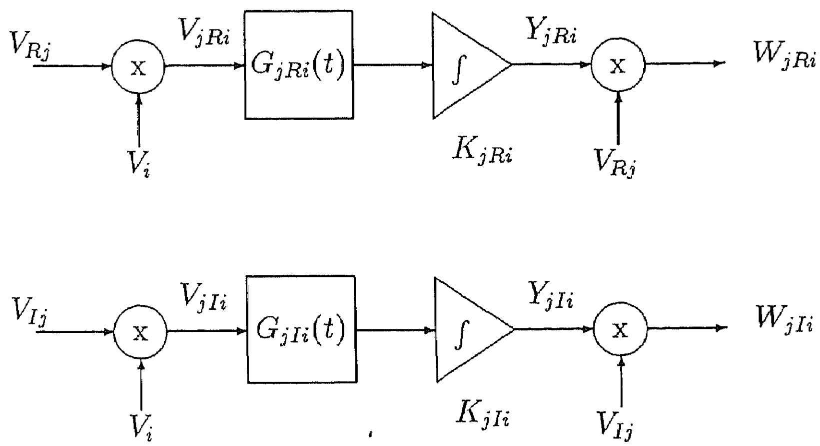

Figure 3.2: Amplitude Control from loop j to loop i

Chapter 4

3CCPLL

In chapter 3, the loop equations and the control equations were developed for the general case of NCCPLL. In this chapter the specific equations for a 3CCPLL are found and simulated using CSMP as a modeling program.

4.1 3CCPLL

Here N=3 and the signal $S(t)$ is composed of 3 signals,

$$S(t) = s_1(t) + s_2(t) + s_3(t) \tag{4.1}$$

where

$$s_1(t) = x_1(t)\sin(w_0 t + \psi_1(t)) \tag{4.2}$$

$$s_2(t) = x_2(t)\sin(w_0 t + \psi_2(t)) \tag{4.3}$$

$$s_3(t) = x_3(t)\sin(w_0 t + \psi_3(t)) \tag{4.4}$$

4.2 Loop Equations

The following three equations are directly deduced from equation (3.11),

$$\begin{aligned}\dot{\Phi}_1(t) &= \alpha_1[\frac{x_1(t)}{A}\sin(\psi_1(t)-\Phi_1(t))+\frac{x_2(t)}{A}\sin(\psi_2(t)-\Phi_1(t))+ \\ &\quad \frac{x_3(t)}{A}\sin(\psi_3(t)-\Phi_1(t))-Y_{2R1}(t)\sin(\Phi_2(t)-\Phi_1(t))- \\ &\quad Y_{2I1}(t)\cos(\Phi_2(t)-\Phi_1(t))-Y_{3R1}(t)\sin(\Phi_3(t)-\Phi_1(t))- \\ &\quad Y_{3I1}(t)\cos(\Phi_3(t)-\Phi_1(t))]*h_1(t) \qquad (4.5)\end{aligned}$$

$$\begin{aligned}\dot{\Phi}_2(t) &= \alpha_2[\frac{x_1(t)}{A}\sin(\psi_1(t)-\Phi_2(t))+\frac{x_2(t)}{A}\sin(\psi_2(t)-\Phi_2(t))+ \\ &\quad \frac{x_3(t)}{A}\sin(\psi_3(t)-\Phi_2(t))-Y_{1R2}(t)\sin(\Phi_1(t)-\Phi_2(t))- \\ &\quad Y_{1I2}(t)\cos(\Phi_1(t)-\Phi_2(t))-Y_{3R2}(t)\sin(\Phi_3(t)-\Phi_2(t))- \\ &\quad Y_{3I2}(t)\cos(\Phi_3(t)-\Phi_2(t))]*h_2(t) \qquad (4.6)\end{aligned}$$

$$\begin{aligned}\dot{\Phi}_3(t) &= \alpha_3[\frac{x_1(t)}{A}\sin(\psi_1(t)-\Phi_3(t))+\frac{x_2(t)}{A}\sin(\psi_2(t)-\Phi_3(t))+ \\ &\quad \frac{x_3(t)}{A}\sin(\psi_3(t)-\Phi_3(t))-Y_{1R3}(t)\sin(\Phi_1(t)-\Phi_3(t))- \\ &\quad Y_{1I3}(t)\cos(\Phi_1(t)-\Phi_3(t))-Y_{2R3}(t)\sin(\Phi_2(t)-\Phi_3(t))- \\ &\quad Y_{2I3}(t)\cos(\Phi_2(t)-\Phi_3(t))]*h_3(t) \qquad (4.7)\end{aligned}$$

Equations (4.5), (4.6) and (4.7) can be written in the following dot product form. From equation (3.16), we have,

$$\begin{aligned}\dot{\Phi}_1(t) &= \alpha_2\begin{bmatrix}\frac{x_1(t)}{A} & \frac{x_2(t)}{A} & \frac{x_3(t)}{A} \\ 0 & Y_{2R1} & Y_{3R1} \\ 0 & Y_{2I1} & Y_{3I1}\end{bmatrix}\bullet \\ &\quad \begin{bmatrix}\sin(\psi_1(t)-\Phi_1(t)) & 0 & 1 \\ \sin(\psi_2(t)-\Phi_1(t)) & \sin(\Phi_2(t)-\Phi_1(t)) & \cos(\Phi_2(t)-\Phi_1(t)) \\ \sin(\psi_3(t)-\Phi_1(t)) & \sin(\Phi_3(t)-\Phi_1(t)) & \cos(\Phi_3(t)-\Phi_1(t))\end{bmatrix}*h_1(t) \qquad (4.8)\end{aligned}$$

$$\dot{\Phi}_2(t) = \alpha_2 \begin{bmatrix} \frac{x_1(t)}{A} & \frac{x_2(t)}{A} & \frac{x_3(t)}{A} \\ Y_{1R2} & 0 & Y_{3R2} \\ Y_{1I2} & 0 & Y_{3I2} \end{bmatrix} \bullet$$
$$\begin{bmatrix} \sin(\psi_1(t) - \Phi_2(t)) & \sin(\Phi_1(t) - \Phi_2(t)) & \cos(\Phi_1(t) - \Phi_2(t)) \\ \sin(\psi_2(t) - \Phi_2(t)) & 0 & 1 \\ \sin(\psi_3(t) - \Phi_2(t)) & \sin(\Phi_3(t) - \Phi_2(t)) & \cos(\Phi_3(t) - \Phi_2(t)) \end{bmatrix} * h_2(t) \tag{4.9}$$

$$\dot{\Phi}_3(t) = \alpha_3 \begin{bmatrix} \frac{x_1(t)}{A} & \frac{x_2(t)}{A} & \frac{x_3(t)}{A} \\ Y_{1R3} & Y_{2R3} & 0 \\ Y_{1I3} & Y_{2I3} & 0 \end{bmatrix} \bullet$$
$$\begin{bmatrix} \sin(\psi_1(t) - \Phi_3(t)) & \sin(\Phi_1(t) - \Phi_3(t)) & \cos(\Phi_1(t) - \Phi_3(t)) \\ \sin(\psi_2(t) - \Phi_3(t)) & \sin(\Phi_2(t) - \Phi_3(t)) & \cos(\Phi_2(t) - \Phi_3(t)) \\ \sin(\psi_3(t) - \Phi_3(t)) & 0 & 1 \end{bmatrix} * h_3(t) \tag{4.10}$$

4.3 Amplitude Control Equations

The following 12 equations are retrieved from equations (3.21) and (3.22).

4.3.1 For Loop 1

$$\begin{aligned} Y_{2R1}(t) = {} & [\frac{x_1(t)}{A}\cos(\psi_1(t) - \Phi_2(t)) + \frac{x_2(t)}{A}\cos(\psi_2(t) - \Phi_2(t)) \\ & \frac{x_3(t)}{A}\cos(\psi_3(t) - \Phi_2(t)) - Y_{3R1}(t)\cos(\Phi_3(t) - \Phi_2(t)) - \\ & Y_{3I1}(t)\sin(\Phi_3(t) - \Phi_2(t))] * F_{2R1}(t) \end{aligned} \tag{4.11}$$

$$
\begin{aligned}
Y_{2I1}(t) &= [\frac{x_1(t)}{A}\sin(\psi_1(t)-\Phi_2(t))+\frac{x_2(t)}{A}\sin(\psi_2(t)-\Phi_2(t)) \\
&\quad \frac{x_3(t)}{A}\sin(\psi_3(t)-\Phi_2(t))-Y_{3R1}(t)\sin(\Phi_3(t)-\Phi_2(t))- \\
&\quad Y_{3I1}(t)\cos(\Phi_3(t)-\Phi_2(t))]*F_{2I1}(t)
\end{aligned}
\tag{4.12}
$$

$$
\begin{aligned}
Y_{3R1}(t) &= [\frac{x_1(t)}{A}\cos(\psi_1(t)-\Phi_3(t))+\frac{x_2(t)}{A}\cos(\psi_2(t)-\Phi_3(t)) \\
&\quad \frac{x_3(t)}{A}\cos(\psi_3(t)-\Phi_3(t))+Y_{2R1}(t)\cos(\Phi_2(t)-\Phi_3(t))- \\
&\quad Y_{2I1}(t)\sin(\Phi_2(t)-\Phi_3(t))]*F_{3R1}(t)
\end{aligned}
\tag{4.13}
$$

$$
\begin{aligned}
Y_{3I1}(t) &= \frac{x_1(t)}{A}\sin(\psi_1(t)-\Phi_3(t))+\frac{x_2(t)}{A}\sin(\psi_2(t)-\Phi_3(t)) \\
&\quad \frac{x_3(t)}{A}\sin(\psi_3(t)-\Phi_3(t))+Y_{2R1}(t)\sin(\Phi_2(t)-\Phi_3(t))- \\
&\quad Y_{2I1}(t)\cos(\Phi_2(t)-\Phi_3(t))]*F_{3I1}(t)
\end{aligned}
\tag{4.14}
$$

Equations (4.11) and (4.12) are the in-phase and quadrature components needed to estimate the amplitude of $s_2(t)$. This estimate is subtracted from the incomming compound signal and, thus, eliminating $s_2(t)$ from the input to loop 1. Equations (4.13) and (4.14) have the same function as the first pair but they estimate and are used to cancel $s_3(t)$.

4.3.2 For Loop 2

$$
\begin{aligned}
Y_{1R2}(t) &= [\frac{x_1(t)}{A}\cos(\psi_1(t)-\Phi_1(t))+\frac{x_2(t)}{A}\cos(\psi_2(t)-\Phi_1(t)) \\
&\quad \frac{x_3(t)}{A}\cos(\psi_3(t)-\Phi_1(t))-Y_{3R2}(t)\cos(\Phi_3(t)-\Phi_1(t))- \\
&\quad Y_{3I2}(t)\sin(\Phi_3(t)-\Phi_1(t))]*F_{1R2}(t)
\end{aligned}
\tag{4.15}
$$

$$
\begin{aligned}
Y_{1I2}(t) \quad = \quad & [\frac{x_1(t)}{A}\sin(\psi_1(t)-\Phi_1(t))+\frac{x_2(t)}{A}\sin(\psi_2(t)-\Phi_1(t)) \\
& \frac{x_3(t)}{A}\sin(\psi_3(t)-\Phi_1(t))-Y_{3R2}(t)\sin(\Phi_3(t)-\Phi_1(t))- \\
& Y_{3I2}(t)\cos(\Phi_3(t)-\Phi_1(t))]*F_{1I2}(t) \qquad (4.16)
\end{aligned}
$$

$$
\begin{aligned}
Y_{3R2}(t) \quad = \quad & [\frac{x_1(t)}{A}\cos(\psi_1(t)-\Phi_3(t))+\frac{x_2(t)}{A}\cos(\psi_2(t)-\Phi_3(t)) \\
& \frac{x_3(t)}{A}\cos(\psi_3(t)-\Phi_3(t))-Y_{1R2}(t)\cos(\Phi_1(t)-\Phi_3(t))- \\
& Y_{1I2}(t)\sin(\Phi_1(t)-\Phi_3(t))]*F_{3R2}(t) \qquad (4.17)
\end{aligned}
$$

$$
\begin{aligned}
Y_{3I2}(t) \quad = \quad & [\frac{x_1(t)}{A}\sin(\psi_1(t)-\Phi_3(t))+\frac{x_2(t)}{A}\sin(\psi_2(t)-\Phi_3(t)) \\
& \frac{x_3(t)}{A}\sin(\psi_3(t)-\Phi_3(t))-Y_{1R2}(t)\sin(\Phi_1(t)-\Phi_3(t))- \\
& Y_{1I2}(t)\cos(\Phi_1(t)-\Phi_3(t))]*F_{3I2}(t) \qquad (4.18)
\end{aligned}
$$

Equations (4.15) and (4.16) are the inphase and quadrature components needed to estimate the amplitude of $s_1(t)$. This estimate is subtracted from the incoming compound signal and, thus, eliminating $s_1(t)$ from the input to loop 2. Equations (4.17) and (4.18) have the same function as the first pair but they estimate and are used to cancel $s_3(t)$.

4.3.3 For Loop 3

$$
\begin{aligned}
Y_{1R3}(t) \quad = \quad & [\frac{x_1(t)}{A}\cos(\psi_1(t)-\Phi_1(t))+\frac{x_2(t)}{A}\cos(\psi_2(t)-\Phi_1(t)) \\
& \frac{x_3(t)}{A}\cos(\psi_3(t)-\Phi_1(t))-Y_{2R3}(t)\cos(\Phi_2(t)-\Phi_1(t))- \\
& Y_{2I3}(t)\sin(\Phi_2(t)-\Phi_1(t))]*F_{1R3}(t) \qquad (4.19)
\end{aligned}
$$

$$\begin{aligned}
Y_{1I3}(t) &= [\frac{x_1(t)}{A}\sin(\psi_1(t)-\Phi_1(t))+\frac{x_2(t)}{A}\sin(\psi_2(t)-\Phi_1(t)) \\
&\quad \frac{x_3(t)}{A}\sin(\psi_3(t)-\Phi_1(t))-Y_{2R3}(t)\sin(\Phi_2(t)-\Phi_1(t))- \\
&\quad Y_{2I3}(t)\cos(\Phi_2(t)-\Phi_1(t))]*F_{1I3}(t) \qquad (4.20)
\end{aligned}$$

$$\begin{aligned}
Y_{2R3}(t) &= [\frac{x_1(t)}{A}\cos(\psi_1(t)-\Phi_2(t))+\frac{x_2(t)}{A}\cos(\psi_2(t)-\Phi_2(t)) \\
&\quad \frac{x_3(t)}{A}\cos(\psi_3(t)-\Phi_2(t))-Y_{1R3}(t)\cos(\Phi_1(t)-\Phi_2(t))- \\
&\quad Y_{1I3}(t)\sin(\Phi_1(t)-\Phi_2(t))]*F_{2R3}(t) \qquad (4.21)
\end{aligned}$$

$$\begin{aligned}
Y_{2I3}(t) &= [\frac{x_1(t)}{A}\sin(\psi_1(t)-\Phi_2(t))+\frac{x_2(t)}{A}\sin(\psi_2(t)-\Phi_2(t)) \\
&\quad \frac{x_3(t)}{A}\sin(\psi_3(t)-\Phi_2(t))-Y_{1R3}(t)\sin(\Phi_1(t)-\Phi_2(t))- \\
&\quad Y_{1I3}(t)\cos(\Phi_1(t)-\Phi_2(t))]*F_{2I3}(t) \qquad (4.22)
\end{aligned}$$

Equations (4.19) and (4.20) are the inphase and quadrature components needed to estimate the amplitude of $s_1(t)$. This estimate is subtracted from the incoming compound signal and, thus, eliminating $s_1(t)$ from the input to loop 3. Equations (4.21) and (4.22) have the same function as the first pair but they estimate and are used to cancel $s_2(t)$.

To use a different perhaps more clear notation, the next 12 equations are the same as equations (4.11) - (4.22) but using the dot product notation,

$$\begin{aligned}
Y_{2R1}(t) &= \begin{bmatrix} \frac{x_1(t)}{A} & \frac{x_2(t)}{A} & \frac{x_3(t)}{A} \\ 0 & Y_{2R1}(t) & Y_{3R1}(t) \\ 0 & Y_{2I1}(t) & Y_{3I1}(t) \end{bmatrix} \bullet \\
&\quad \begin{bmatrix} \cos(\psi_1(t)-\Phi_2(t)) & \cos(\Phi_1(t)-\Phi_2(t)) & \sin(\Phi_1(t)-\Phi_2(t)) \\ \cos(\psi_2(t)-\Phi_2(t)) & 0 & 0 \\ \cos(\psi_3(t)-\Phi_2(t)) & \cos(\Phi_3(t)-\Phi_2(t)) & \sin(\Phi_3(t)-\Phi_2(t)) \end{bmatrix} * F_{2R1}(t) \qquad (4.23)
\end{aligned}$$

$$Y_{2I1}(t) = \begin{bmatrix} \frac{x_1(t)}{A} & \frac{x_2(t)}{A} & \frac{x_3(t)}{A} \\ 0 & Y_{2R1}(t) & Y_{3R1}(t) \\ 0 & Y_{2I1}(t) & Y_{3I1}(t) \end{bmatrix} \bullet$$
$$\begin{bmatrix} \sin(\psi_1(t)-\Phi_2(t)) & \sin(\Phi_1(t)-\Phi_2(t)) & \cos(\Phi_1(t)-\Phi_2(t)) \\ \sin(\psi_2(t)-\Phi_2(t)) & 0 & 0 \\ \sin(\psi_3(t)-\Phi_2(t)) & \sin(\Phi_3(t)-\Phi_2(t)) & \cos(\Phi_3(t)-\Phi_2(t)) \end{bmatrix} * F_{2I1}(t) \tag{4.24}$$

$$Y_{3R1}(t) = \begin{bmatrix} \frac{x_1(t)}{A} & \frac{x_2(t)}{A} & \frac{x_3(t)}{A} \\ 0 & Y_{2R1}(t) & Y_{3R1}(t) \\ 0 & Y_{2I1}(t) & Y_{3I1}(t) \end{bmatrix} \bullet$$
$$\begin{bmatrix} \cos(\psi_1(t)-\Phi_3(t)) & \cos(\Phi_1(t)-\Phi_3(t)) & \sin(\Phi_1(t)-\Phi_3(t)) \\ \cos(\psi_2(t)-\Phi_3(t)) & \cos(\Phi_2(t)-\Phi_3(t)) & \sin(\Phi_2(t)-\Phi_3(t)) \\ \cos(\psi_3(t)-\Phi_3(t)) & 0 & 0 \end{bmatrix} * F_{3R1}(t) \tag{4.25}$$

$$Y_{3I1}(t) = \begin{bmatrix} \frac{x_1(t)}{A} & \frac{x_2(t)}{A} & \frac{x_3(t)}{A} \\ 0 & Y_{2R1}(t) & Y_{3R1}(t) \\ 0 & Y_{2I1}(t) & Y_{3I1}(t) \end{bmatrix} \bullet$$
$$\begin{bmatrix} \sin(\psi_1(t)-\Phi_3(t)) & \sin(\Phi_1(t)-\Phi_3(t)) & \cos(\Phi_1(t)-\Phi_3(t)) \\ \sin(\psi_2(t)-\Phi_3(t)) & \sin(\Phi_2(t)-\Phi_3(t)) & \cos(\Phi_2(t)-\Phi_3(t)) \\ \sin(\psi_3(t)-\Phi_3(t)) & 0 & 0 \end{bmatrix} * F_{3I1}(t) \tag{4.26}$$

$$Y_{1R2}(t) = \begin{bmatrix} \frac{x_1(t)}{A} & \frac{x_2(t)}{A} & \frac{x_3(t)}{A} \\ Y_{1R2}(t) & 0 & Y_{3R2}(t) \\ Y_{1I2}(t) & 0 & Y_{3I2}(t) \end{bmatrix} \bullet$$
$$\begin{bmatrix} \cos(\psi_1(t)-\Phi_1(t)) & 0 & 0 \\ \cos(\psi_2(t)-\Phi_1(t)) & \cos(\Phi_2(t)-\Phi_1(t)) & \sin(\Phi_2(t)-\Phi_1(t)) \\ \cos(\psi_3(t)-\Phi_1(t)) & \cos(\Phi_3(t)-\Phi_1(t)) & \sin(\Phi_3(t)-\Phi_1(t)) \end{bmatrix} * F_{1R2}(t) \tag{4.27}$$

$$Y_{1I2}(t) = \begin{bmatrix} \dfrac{x_1(t)}{A} & \dfrac{x_2(t)}{A} & \dfrac{x_3(t)}{A} \\ Y_{1R2}(t) & 0 & Y_{3R1}(t) \\ Y_{1I2}(t) & 0 & Y_{3I1}(t) \end{bmatrix} \bullet \begin{bmatrix} \sin(\psi_1(t) - \Phi_1(t)) & 0 & 0 \\ \sin(\psi_2(t) - \Phi_1(t)) & \sin(\Phi_2(t) - \Phi_1(t)) & \cos(\Phi_2(t) - \Phi_1(t)) \\ \sin(\psi_3(t) - \Phi_1(t)) & \sin(\Phi_3(t) - \Phi_1(t)) & \cos(\Phi_3(t) - \Phi_1(t)) \end{bmatrix} * F_{1I2}(t) \tag{4.28}$$

$$Y_{3R2}(t) = \begin{bmatrix} \dfrac{x_1(t)}{A} & \dfrac{x_2(t)}{A} & \dfrac{x_3(t)}{A} \\ Y_{1R2}(t) & 0 & Y_{3R2}(t) \\ Y_{1I2}(t) & 0 & Y_{3I2}(t) \end{bmatrix} \bullet \begin{bmatrix} \cos(\psi_1(t) - \Phi_3(t)) & \cos(\Phi_1(t) - \Phi_3(t)) & \sin(\Phi_1(t) - \Phi_3(t)) \\ \cos(\psi_2(t) - \Phi_3(t)) & \cos(\Phi_2(t) - \Phi_3(t)) & \sin(\Phi_2(t) - \Phi_3(t)) \\ \cos(\psi_3(t) - \Phi_3(t)) & 0 & 0 \end{bmatrix} * F_{3R2}(t) \tag{4.29}$$

$$Y_{3I2}(t) = \begin{bmatrix} \dfrac{x_1(t)}{A} & \dfrac{x_2(t)}{A} & \dfrac{x_3(t)}{A} \\ Y_{1R2}(t) & 0 & Y_{3R2}(t) \\ Y_{1I2}(t) & 0 & Y_{3I2}(t) \end{bmatrix} \bullet \begin{bmatrix} \sin(\psi_1(t) - \Phi_3(t)) & \sin(\Phi_1(t) - \Phi_3(t)) & \cos(\Phi_1(t) - \Phi_3(t)) \\ \sin(\psi_2(t) - \Phi_3(t)) & \sin(\Phi_2(t) - \Phi_3(t)) & \cos(\Phi_2(t) - \Phi_3(t)) \\ \sin(\psi_3(t) - \Phi_3(t)) & 0 & 0 \end{bmatrix} * F_{3I2}(t) \tag{4.30}$$

$$Y_{1R3}(t) = \begin{bmatrix} \dfrac{x_1(t)}{A} & \dfrac{x_2(t)}{A} & \dfrac{x_3(t)}{A} \\ Y_{1R3}(t) & Y_{2R3}(t) & 0 \\ Y_{1I3}(t) & Y_{2I3}(t) & 0 \end{bmatrix} \bullet \begin{bmatrix} \cos(\psi_1(t) - \Phi_1(t)) & 0 & 0 \\ \cos(\psi_2(t) - \Phi_1(t)) & \cos(\Phi_2(t) - \Phi_1(t)) & \sin(\Phi_2(t) - \Phi_1(t)) \\ \cos(\psi_3(t) - \Phi_1(t)) & \cos(\Phi_3(t) - \Phi_1(t)) & \sin(\Phi_3(t) - \Phi_1(t)) \end{bmatrix} * F_{1R3}(t) \tag{4.31}$$

$$
\begin{aligned}
Y_{1I3}(t) &= \begin{bmatrix} \dfrac{x_1(t)}{A} & \dfrac{x_2(t)}{A} & \dfrac{x_3(t)}{A} \\ Y_{1R3}(t) & Y_{2R3}(t) & 0 \\ Y_{1I3}(t) & Y_{2I3}(t) & 0 \end{bmatrix} \bullet \\
&\begin{bmatrix} \sin(\psi_1(t)-\Phi_1(t)) & 0 & 0 \\ \sin(\psi_2(t)-\Phi_1(t)) & \sin(\Phi_2(t)-\Phi_1(t)) & \cos(\Phi_2(t)-\Phi_1(t)) \\ \sin(\psi_3(t)-\Phi_1(t)) & \sin(\Phi_3(t)-\Phi_1(t)) & \cos(\Phi_3(t)-\Phi_1(t)) \end{bmatrix} * F_{1I3}(t)
\end{aligned} \tag{4.32}
$$

$$
\begin{aligned}
Y_{2R3}(t) &= \begin{bmatrix} \dfrac{x_1(t)}{A} & \dfrac{x_2(t)}{A} & \dfrac{x_3(t)}{A} \\ Y_{1R3}(t) & Y_{2R3}(t) & 0 \\ Y_{1I3}(t) & Y_{2I3}(t) & 0 \end{bmatrix} \bullet \\
&\begin{bmatrix} \cos(\psi_1(t)-\Phi_2(t)) & \cos(\Phi_1(t)-\Phi_2(t)) & \sin(\Phi_1(t)-\Phi_2(t)) \\ \cos(\psi_2(t)-\Phi_2(t)) & 0 & 0 \\ \cos(\psi_3(t)-\Phi_2(t)) & \cos(\Phi_3(t)-\Phi_2(t)) & \sin(\Phi_3(t)-\Phi_2(t)) \end{bmatrix} * F_{2R3}(t)
\end{aligned} \tag{4.33}
$$

$$
\begin{aligned}
Y_{2I3}(t) &= \begin{bmatrix} \dfrac{x_1(t)}{A} & \dfrac{x_2(t)}{A} & \dfrac{x_3(t)}{A} \\ Y_{1R3}(t) & Y_{2R3}(t) & 0 \\ Y_{1I3}(t) & Y_{2I3}(t) & 0 \end{bmatrix} \bullet \\
&\begin{bmatrix} \sin(\psi_1(t)-\Phi_2(t)) & \sin(\Phi_1(t)-\Phi_2(t)) & \cos(\Phi_1(t)-\Phi_2(t)) \\ \sin(\psi_2(t)-\Phi_2(t)) & 0 & 0 \\ \sin(\psi_3(t)-\Phi_2(t)) & \sin(\Phi_3(t)-\Phi_2(t)) & \cos(\Phi_3(t)-\Phi_2(t)) \end{bmatrix} * F_{2I3}(t)
\end{aligned} \tag{4.34}
$$

Chapter 5

SIMULATION RESULTS

The first objective was to determine whether or not lock, separation and demodulation occur on each PLL. The three FM signals that served as input to the 3CC-PLL are at three very close carrier frequencies ($FC1 = 1000Hz$, $FC2 = 1010Hz$, $FC3 = 990Hz$). Thus, the 3 FM signals occupied the same frequency band. Each of the FM signals carried a message. Figure 5.1 shows the steady state output of all 3 PLLs. It is apparent that separation and demodulation were successful. The power ratios of the three signals were [4:2.25:1].

The three messages where sine waves with respective frequencies $10Hz$, $20Hz$, and $15Hz$ and modulation was chosen to have 10 as an index of modulation. The three carriers were changed in such a manner to come closer to each other as well as equal each other. The output stayed the same as in figure 5.1. For this simulation, the system blocks rather than the final derived equations were simulated using CSMP (See Appendix B). The reason fo this is that the derived equations assume that all carrier frequencies are the same, thus, different carrier frequencies cannot be simulated through the the derived equations.

The second objective was to determine how long it would take the CCPLL to lock and what, if any, is the relation between power ratios and acquisition time. Figure 5.2 shows the result of simulation in the case of 3CCPLL. Here, in order to illustrate the acquisition time, the interferers carried no messages and they were at the same carrier frequency as that of the desired FM signal. The ratios of interferers to desired signal are [49:9:1]. In this exercise, equations (4.5) - (4.7) and (4.11) - (4.22) were simulated using CSMP. The amplitude control signals for this case are shown in figure 5.3. It is evident that all three signals start at the same value and end up at different steady state values. Also, in figure 5.2 $\Phi_1(t)$ and $\Phi_2(t)$ are exactly equal and very small. In figure 5.3 qab denotes the squareroot of the sum of squares of the in phase and quadrature components of the amplitude control. The disturbances in the amplitude control signals correspond to the time when the instintaneous frequencies of the three carriers cross.

Figure 5.4 is the same as figure 5.2 with [196:36:1] as power ratios. It is evident that the higher the power ratio the longer the acquisition time. This is reasonable since it would be harder to detect lower power signals burried under higher power interferers. The amplitude control corresponding to figure 5.4 are shown in figure 5.5. In order to show the relation between power and acquisition time, figure 5.6 shows a plot of the latter versus the former. Here, one of the interferers was fixed at a certain power (4W) and the other was changed from 16W to 74W while the message carrier was 1W.

For the CCPLL to work, the filter $F_i(t)$ in the control circuit has to be of narrow bandwidth to include $x_i(t)\cos(\psi_i(t)-\Phi_i(t))$ but not $x_i(t)\cos(\psi_i(t)-\Phi_j(t))$. A plot of acquisition time versus filter bandwidth is dipicted in figure 5.7. It can be seen that it takes a long time to enter the tracking mode if the bandwidth is small. For example, with a message that has the bandwidth of 1rd, if the filter bandwidth is 3rd it takes about 17s to enter the tracking mode. However, if the filter bandwidth is 30rd it takes around 5s. For $BW > 200$ rd the acquisition is constant. This can be explained by pointing out that the smaller the filter bandwidth the less the information (in this case power, and therefore amplitude) is available to correctly estimate the magnitude. What figure 5.7 does not show is that the acquisition time should increase again when the bandwidth of the filter gets close to the frequency range of $x_i(t)\cos(\psi_i(t)-\Phi_j(t))$. This is so because in our simulation $\psi_j(t)$ was set to zero.

Figure 5.8 illustrates the capture effect of PLL. Here, the message amplitude was switched with that of the interferer with the lowest amplitude. Thus, the desired signal power is in between that of the two interferers. Figure 4.6 shows that the message is now received on PLL #2 rather than PLL #3 as was the case in figure 4.2 when the desired message had the lowest power. Also notice that here the acquisition time is very close to 0, although one interferer is still larger than the desired FM signal.

Future work in this area should include the analysis of the NCCPLL in a noisy environment as well as stability considerations and the probabilityies of cycle slipping and sync failure.

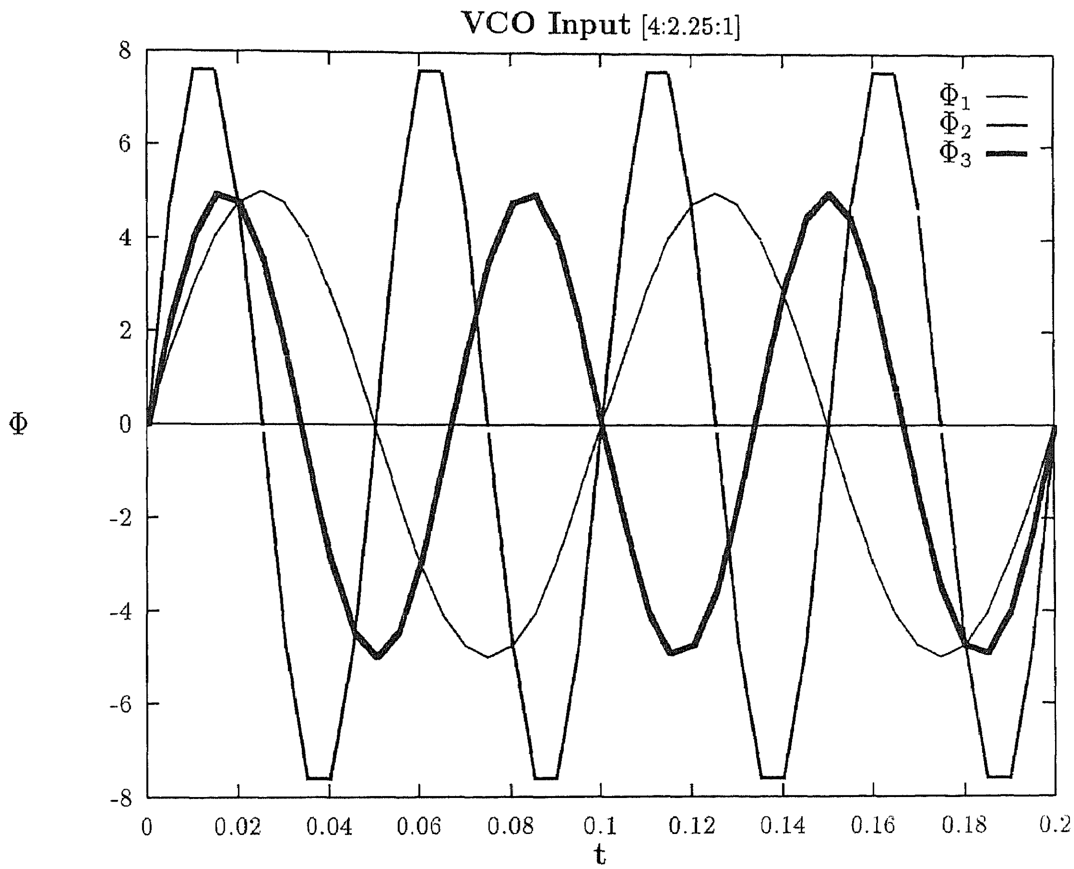

Figure 5.1: The input to the VCO of loop 1, 2, and 3 for the case of 3 FM signals with messages

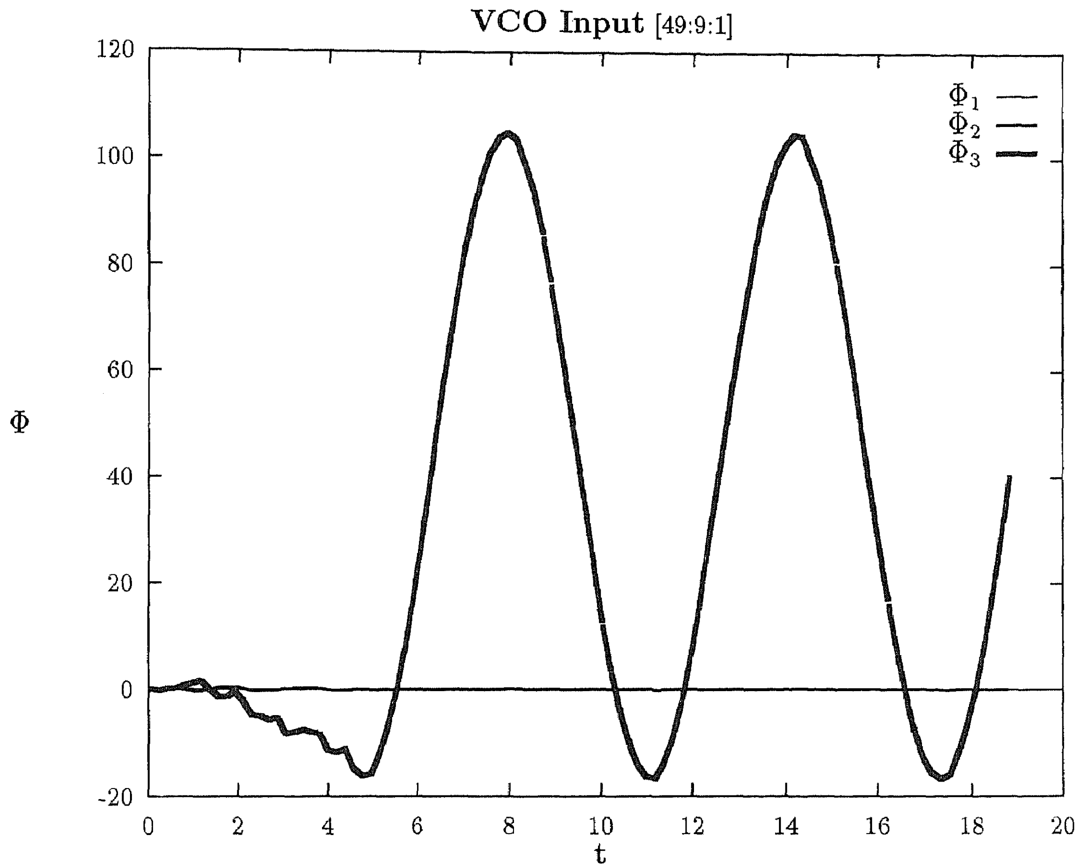

Figure 5.2: The case of 1 FM signal and 2 interferers with no messages.

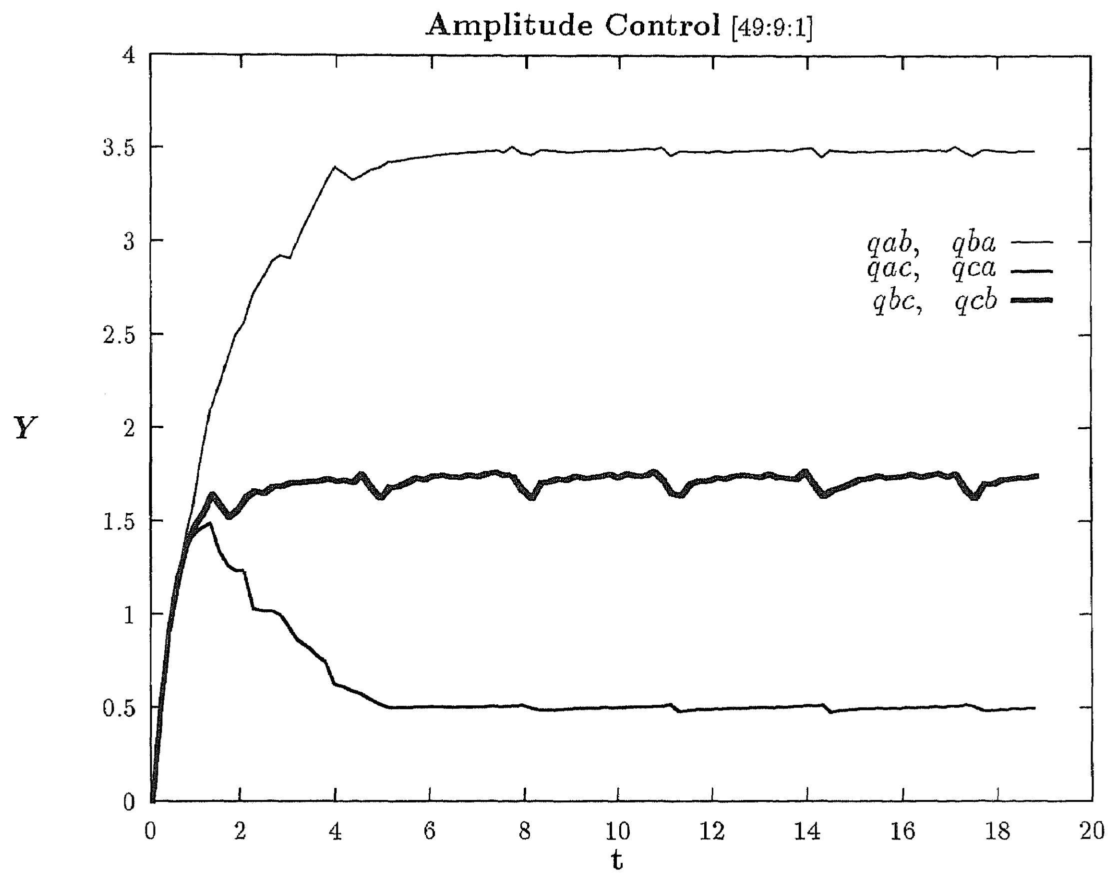

Figure 5.3: Amplitude control estimates for figure 5.2.

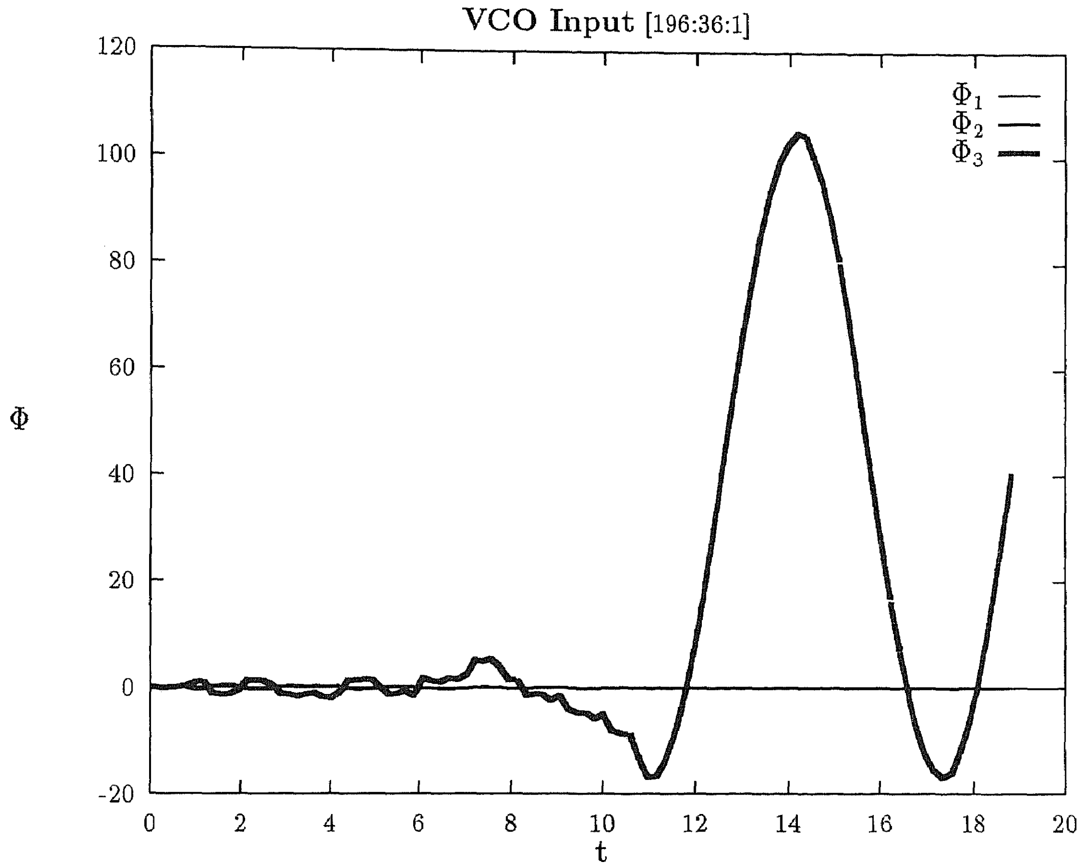

Figure 5.4: Same as figure 5.2 but power ratio is different.

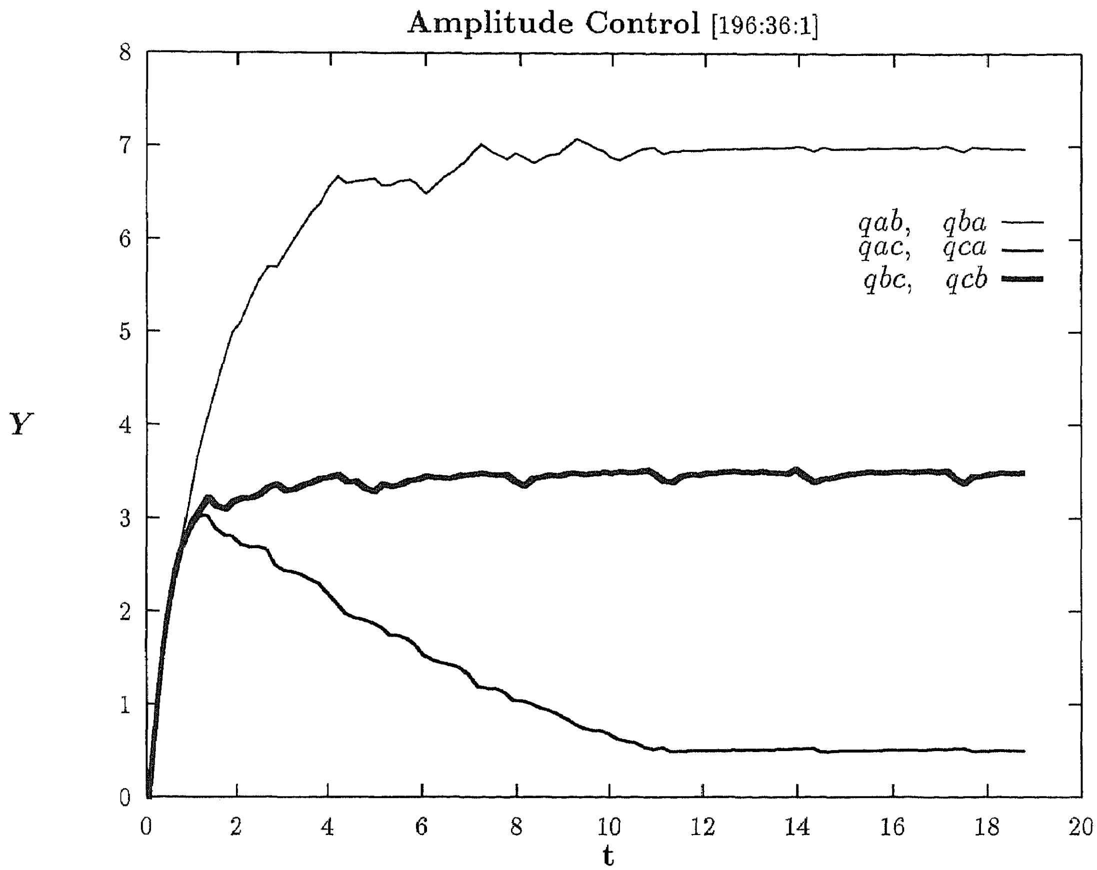

Figure 5.5: Amplitude control estimates for figure 5.4.

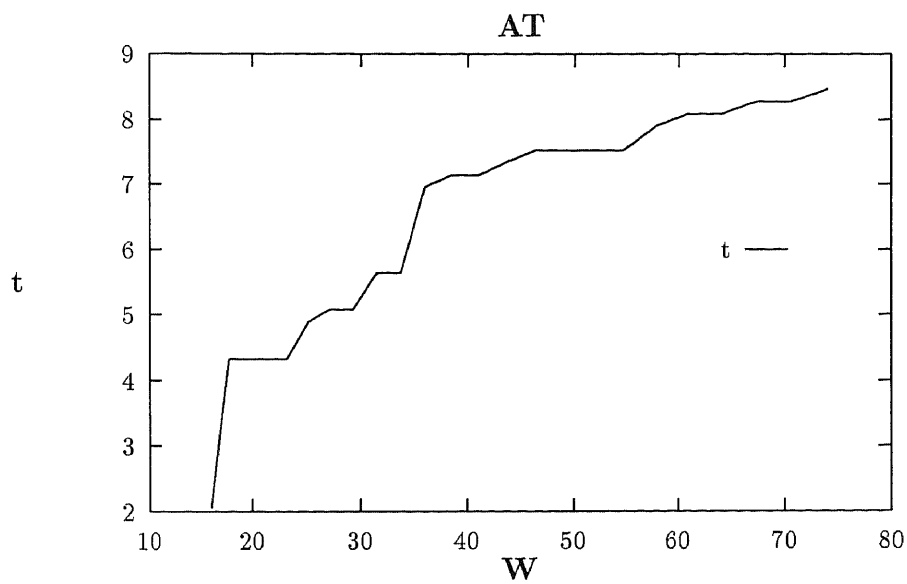

Figure 5.6: Acquisition time versus power ratio.

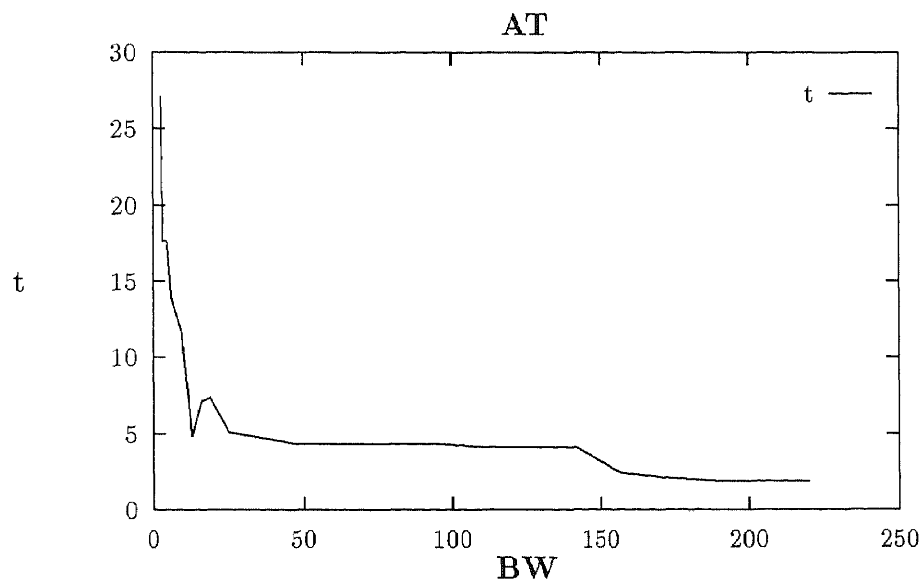

Figure 5.7: Acquisition time versus filter bandwidth.

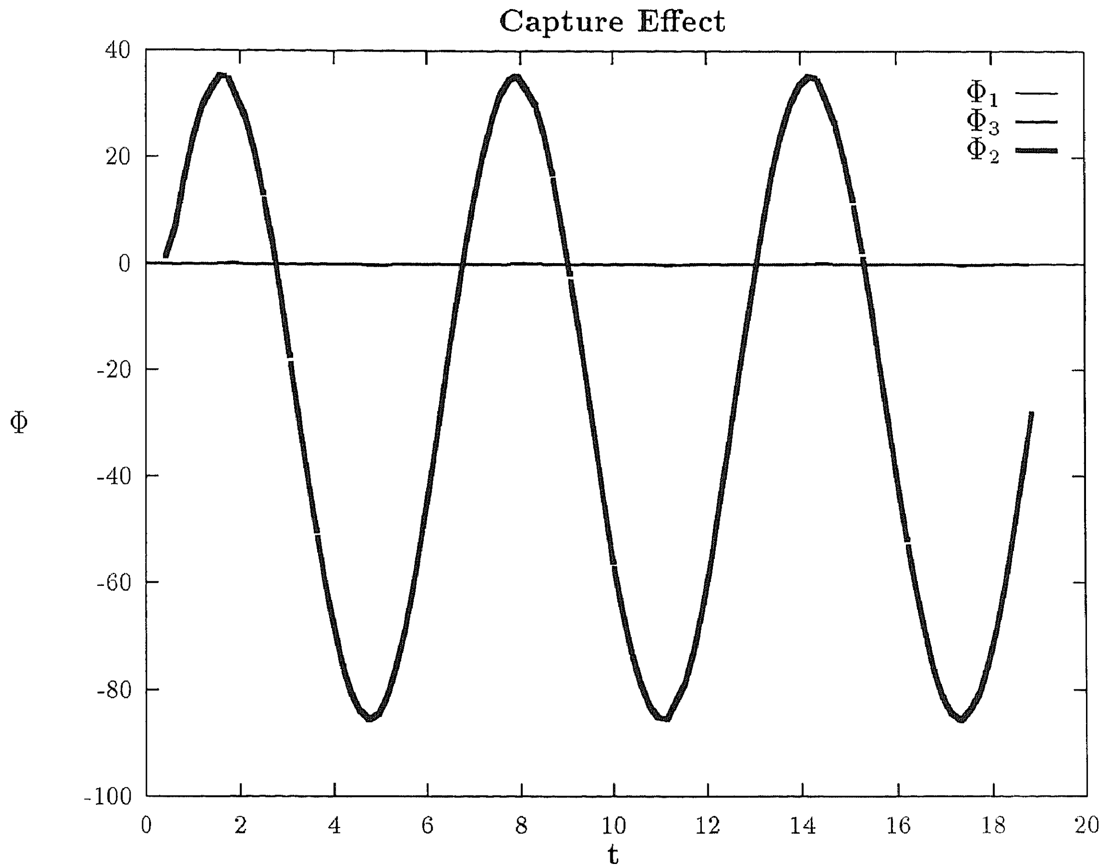

Figure 5.8: Capture effect is illustrated by the switch from loop three in figure 5.2 to loop 2 in this figure.

Appendix A

Narrowband Gaussian Process

Let $n_s(t)$ and $n_c(t)$ be two narrowband zero-mean Gaussian random processes. One can form a new process of the form

$$n_i(t) = \sqrt{2}(n_c(t)\cos(w_0 t) - n_s(t)\sin(w_0 t)) \tag{A.1}$$

This process can also be written in its polar form

$$\begin{aligned} n_i(t) &= \sqrt{2}N_i(t)\cos\phi_i(t) & \text{(A.2)} \\ &= \sqrt{2}N_i(t)\cos(w_0(t) + \theta_i(t)) & \text{(A.3)} \end{aligned}$$

where $N_i(t)$ and $\theta_i(t)$ are the envelope and phase of the $n_i(t)$. It is apparent that,

$$\begin{aligned} n_c(t) &= N_i(t)\cos\theta_i(t) \\ n_s(t) &= N_i(t)\sin\theta_i(t) \end{aligned}$$

The autocorrelation function $R_{n_i}(t, t+\tau)$ is defined as,

$$R_{n_i}(t, t+\tau) = E[(n(t)n(t+\tau)] \tag{A.4}$$

Therefore,

$$
\begin{aligned}
R_{ni}(t, t+\tau) &= 2E[(n_c(t)\cos(w_0 t) - n_s(t)\sin(w_0 t)) \\
&\quad (n_c(t+\tau)\cos(w_0(t+\tau)) - n_s(t+\tau)\sin(w_0(t+\tau)))] \qquad \text{(A.5)} \\
&= \{E[n_c(t)n_c(t+\tau)]\cos(w_0\tau) - E[n_c(t)n_s(t+\tau)]\sin(w_0\tau) \\
&\quad + E[n_s(t)n_c(t+\tau)]\sin(w_0\tau) + E[n_s(t)n_s(t+\tau)]\cos(w_0\tau) \\
&\quad + E[n_c(t)n_c(t+\tau)]\cos(w_0(2t+\tau)) \\
&\quad - E[n_c(t)n_s(t+\tau)]\sin(w_0(2t+\tau)) \\
&\quad - E[n_s(t)n_c(t+\tau)]\sin(w_0(2t+\tau)) \\
&\quad - E[n_s(t)n_s(t+\tau)]\cos(w_0(2t+\tau))\}
\end{aligned}
$$

This process is stationary if and only if

$$
\begin{aligned}
E[n_c(t)n_c(t+\tau)] &= E[n_s(t)n_s(t+\tau)] && \text{(A.6)} \\
E[n_c(t)n_s(t+\tau)] &= -E[n_s(t)n_c(t+\tau)] && \text{(A.7)}
\end{aligned}
$$

Thus, under these conditions, $R_{n_i}(t, t+\tau) = R_{n_i}(\tau)$ and hence,

$$
\begin{aligned}
R_{n_i}(\tau) &= 2E[n_c(t)n_c(t+\tau)]\cos(w_0\tau) \\
&\quad - 2E[n_c(t)n_s(t+\tau)]\sin(w_0\tau) && \text{(A.8)} \\
&= 2r(\tau)\cos(w_0\tau) - 2q(\tau)\sin(w_0\tau) && \text{(A.9)}
\end{aligned}
$$

where

$$
\begin{aligned}
r(\tau) &= E[n_c(t)n_c(t+\tau)] && \text{(A.10)} \\
q(\tau) &= E[n_c(t)n_s(t+\tau)] && \text{(A.11)}
\end{aligned}
$$

If the processes $n_c(t)$ and $n_s(t)$ are uncorrelated, then $q(\tau) = 0$ and the autocorrelation of $n_i(t)$ becomes,

$$R_{n_i}(\tau) = 2r(\tau)\cos(w_0\tau) \qquad \text{(A.12)}$$

Appendix B

Program 1

This is a program to simulate a 3CCPLL system that can separate 3 FM signals and demodulate their messages.
In this program the following notations will be used:

- A1, A2, A3 are the messages amplitudes.
- AC1, AC2, AC3 are the FM carriers powers.
- WC1, WC2, WC3 are the carriers frequencies.
- W1, W2, W3 are the messages frequencies.
- KF1, KF2, KF3 are the frequency deviation constants.
- WV1, WV2, WV3 are the VCO center frequencies.
- KV1, KV2, KV3 are the loop gains.
- KV/T1, 1/T2 are the loop filter break frequencies.
- 1/P is the control circuit filter break frequency.

```
INITIAL
NOSORT
          CONSTANT A1=5.0, A2=8.0, A3=5.0,
          CONSTANT AC1 =20.0, AC2=10.0, AC3=15.0
          CONSTANT WC1 = 6283.19, WC2 = 6346.0, WC3 = 6220.35
          CONSTANT W1 = 62.83, W2 = 125.66, W3 = 94.25
          CONSTANT KF1 = 125.66, KF2 = 157.08, KF3 = 188.5
          CONSTANT B1 = 1, B2 = 1, B3 = 1, T1 = 62.8, T2 = 0.02
          CONSTANT WV1 = 6283.19, WV2 = 6346.0, WV3 = 6220.35
          CONSTANT KV1 = 100000, KV2 = 100000, KV3 = 100000,
          CONSTANT P = 0.01, PIE = 1.571
DYNAMIC
NOSORT
          PS1 = A1 * SINE(0.0,W1,0.0)
          PS2 = A2 * SINE(0.0,W2,0.0)
          PS3 = A3 * SINE(0.0,W3,0.0)
          FM1 = KF1 * INTGRL(0.0,PS1)
          FM2 = KF2 * INTGRL(0.0,PS2)
          FM3 = KF3 * INTGRL(0.0,PS3)
          FM1I = FM1 + PIE
          FM2I = FM2 + PIE
          FM3I = FM3 + PIE
          TEM1A = SINE(0.0,WC1,0.0) * SIN(FM1I)
          TEM1B = SINE(0.0,WC1,PIE) * SIN(FM1)
          TEM1C = TEM1A + TEM1B
          TEM2A = SINE(0.0,WC2,0.0) * SIN(FM2I)
          TEM2B = SINE(0.0,WC2,PIE) * SIN(FM2)
          TEM2C = TEM2A + TEM2B
          TEM3A = SINE(0.0,WC3,0.0) * SIN(FM3I)
          TEM3B = SINE(0.0,WC3,PIE) * SIN(FM3)
          TEM3C = TEM3A + TEM3B
          S1 = AC1 * TEM1C
          S2 = AC2 * TEM2C
          S3 = AC3 * TEM3C
```

```
        V = S1 + S2 + S3
SORT
        CV1 = Y2R1*V2ER + Y2I1*V2E + Y3R1*V3ER +
                Y3I1*V3E
        CV2 = Y1R2*V1ER + Y1I2*V1E + Y3R2*V3ER +
                Y3I2*V3E
        CV3 = Y1R3*V1ER + Y1I3*V1E + Y2R3*V2ER +
                Y2I3*V2E
        V1 = V - CV1
        V2 = V - CV2
        V3 = V - CV3
        X1 = V1 * V1E
        X2 = V2 * V2E
        X3 = V3 * V3E
        PH1 = (1/T1)*(T2 * X1 + INTGRL(0.0,X1))
        PH2 = (1/T1)*(T2 * X2 + INTGRL(0.0,X2))
        PH3 = (1/T1)*(T2 * X3 + INTGRL(0.0,X3))
        TEMP1 = KV1 * INTGRL(0.0,PH1)
        TEMP2 = KV2 * INTGRL(0.0,PH2)
        TEMP3 = KV3 * INTGRL(0.0,PH3)
        TEMP1I = TEMP1 + PIE
        TEMP2I = TEMP2 + PIE
        TEMP3I = TEMP3 + PIE
        TE1C = SINE(0.0,WV1,TEMP1)
        TE2C = SINE(0.0,WV2,TEMP2)
        TE3C = SINE(0.0,WV3,TEMP3)
        TE1CI = SINE(0.0,WV1,TEMP1I)
        TE2CI = SINE(0.0,WV2,TEMP2I)
        TE3CI = SINE(0.0,WV3,TEMP3I)
        V1E = B1 * TE1CI
        V2E = B2 * TE2CI
        V3E = B3 * TE3CI
        V1ER = B1 * TE1C
        V2ER = B2 * TE2C
        V3ER = B3 * TE3C
```

```
DVC1R2 = V2 * V1ER
DVC1I2 = V2 * V1E
DVC1R3 = V3 * V1ER
DVC1I3 = V3 * V1E
DVC2R1 = V1 * V2ER
DVC2I1 = V1 * V2E
DVC2R3 = V3 * V2ER
DVC2I3 = V3 * V2E
DVC3R1 = V1 * V3ER
DVC3I1 = V1 * V3ER
DVC3R2 = V2 * V3ER
DVC3I2 = V2 * V3E
VC1R2 = INTGRL(0.0,DVC1R2)
VC1R3 = INTGRL(0.0,DVC1R3)
VC2R1 = INTGRL(0.0,DVC2R1)
VC2R3 = INTGRL(0.0,DVC2R3)
VC3R1 = INTGRL(0.0,DVC3R1)
VC3R2 = INTGRL(0.0,DVC3R2)
VC1I2 = INTGRL(0.0,DVC1R2)
VC1I3 = INTGRL(0.0,DVC1R3)
VC2I1 = INTGRL(0.0,DVC2R1)
VC2I3 = INTGRL(0.0,DVC2R3)
VC3I1 = INTGRL(0.0,DVC3R1)
VC3I2 = INTGRL(0.0,DVC3R2)
Y2R1 = REALPL(0.0,P,VC2R1)
Y2I1 = REALPL(0.0,P,VC2I1)
Y2R3 = REALPL(0.0,P,VC2R3)
Y2I3 = REALPL(0.0,P,VC2I3)
Y1R2 = REALPL(0.0,P,VC1R2)
Y1I2 = REALPL(0.0,P,VC1I2)
Y1R3 = REALPL(0.0,P,VC1R3)
Y1I3 = REALPL(0.0,P,VC1I3)
Y3R1 = REALPL(0.0,P,VC3R1)
Y3I1 = REALPL(0.0,P,VC3I1)
Y3I2 = REALPL(0.0,P,VC3I2)
```

```
TERMINAL
NOSORT
          TIMER FINTIM = 0.5, OUTDEL = 0.005, DELMIN = 1.0E-14
          PRINT PS1, PS2, PS3
          END
          STOP
ENDJOB
```

Appendix C

Program 2

The following is a program to simulate equations (4.8) - (4.10) and (4.23) - (4.34). In this program the following definitions are assumed:

- A1, A2 and A3 are the gains for loop filters of PLL # 1, 2 and 3 respectively.
- B1, B2 and B3 are the gains for the amplitude control filters.
- ZA1, ZA2 and ZA3 are the VCO constants.
- LR and LI are the break frequencies for the amplitude control filters.
- XA, XB and XC are the input amplitudes of the FM signals.
- SA, SB and SC are the modulating phases of the FM signals.
- VCO1I, VCO2I and VCO3I are the inputs to the VCOs of loop 1,2 and 3 respectively.
- SQAB, SQAC, AQBA, SQBC, SQCA and SQCB are the amplitude estimates as in equation (3.38).

```
CONSTANT A1 = 5, A2 = 5, A3 = 60
CONSTANT B1 = 1.0, B2 = 1.0, B3 = 1.0
CONSTANT ZA1 = 20, ZA2 = 30, ZA3 = 10
CONSTANT LR = 100, LI = 100
ILI = 1 / LI
ILR = 1 / LR
XA = 2.0
XB = 1.5
XC = 0.5
SA = 0.0
SB = 0.0
SC = 60*SINE(0.0,1.0,0.0)
F1 = XA*SIN(SA - YA) + XB*SIN(SB - YA) + XC*SIN(SC - YA)
F2 = XA*SIN(SA - YB) + XB*SIN(SB - YB) + XC*SIN(SC - YB)
F3 = XA*SIN(SA - YC) + XB*SIN(SB - YC) + XC*SIN(SC - YC)
F4 = ARB*SIN(YB - YA) + AIB*COS(YB - YA) + ARC*SIN(YC - YA) +
        AIC*COS(YC - YA)
F5 = BRA*SIN(YA - YB) + BIA*COS(YA - YB) + BRC*SIN(YC - YB) +
        BIC*COS(YC - YB)
F6 = CRA*SIN(YA - YC) + CIA*COS(YA - YC) + CRB*SIN(YB - YC) +
        CIB*COS(YB - YC)
F14 = F1 - F4
F25 = F2 - F5
F36 = F3 - F6
VCO1I = A1*(F14 + ZA1*INTGRL(0.0,F14))
VCO2I = A2*(F25 + ZA2*INTGRL(0.0,F25))
VCO3I = A3*(F36 + ZA3*INTGRL(0.0,F36))
YA = INTGRL(0.0,VCO1I)
YB = INTGRL(0.0,VCO2I)
YC = INTGRL(0.0,VCO3I)
FAIB = B2*(F2 - ARC*SIN(YC - YB) - AIC*COS(YC - YB) - AIB)
FAIC = B3*(F3 - ARB*SIN(YB - YC) - AIB*COS(YB - YC) - AIC)
FBIA = B1*(F1 - BRC*SIN(YC - YA) - BIC*COS(YC - YA) - BIA)
FBIC = B3*(F3 - BRA*SIN(YA - YC) - BIA*COS(YA - YC) - BIC)
FCIA = B1*(F1 - CRB*SIN(YB - YA) - CIB*COS(YB - YA) - CIA)
```

```
FCIB = B2*(F2 - CRA*SIN(YA - YB) - CIA*COS(YA - YB) - CIB)
FARB = B2*(XA*COS(SA - YB) + XB*COS(SB - YB) + XC*COS(SC
        - YB) - ARC*COS(YC - YB) - AIC*SIN(YC - YB) - ARB)
FARC = B3*(XA*COS(SA - YC) + XB*COS(SB - YC) + XC*COS(SC
        - YC) - ARB*COS(YB - YC) - AIB*SIN(YB - YC) - ARC)
FBRA = B1*(XA*COS(SA - YA) + XB*COS(SB - YA) + XC*COS(SC
        - YA) - BRC*COS(YC - YA) - BIC*SIN(YC - YA) - BRA)
FBRC = B3*(XA*COS(SA - YC) + XB*COS(SB - YC) + XC*COS(SC
        - YC) - BRA*COS(YA - YC) - BIA*SIN(YA - YC) - BRC)
FCRA = B1*(XA*COS(SA - YA) + XB*COS(SB - YA) + XC*COS(SC
        - YA) - CRB*COS(YB - YA) - CIB*SIN(YB - YA) - CRA)
FCRB = B2*(XA*COS(SA - YB) + XB*COS(SB - YB) + XC*COS(SC
        - YB) - CRA*COS(YA - YB) - CIA*SIN(YA - YB) - CRB)
AIBDOT = REALPL(0.0,ILI,FAIB)
AICDOT = REALPL(0.0,ILI,FAIC)
BIADOT = REALPL(0.0,ILI,FBIA)
BICDOT = REALPL(0.0,ILI,FBIC)
CIADOT = REALPL(0.0,ILI,FCIA)
CIBDOT = REALPL(0.0,ILI,FCIB)
ARBDOT = REALPL(0.0,ILR,FARB)
ARCDOT = REALPL(0.0,ILR,FARC)
BRADOT = REALPL(0.0,ILR,FBRA)
BRCDOT = REALPL(0.0,ILR,FBRC)
CRADOT = REALPL(0.0,ILR,FCRA)
CRBDOT = REALPL(0.0,ILR,FCRB)
AIB = INTGRL(0.0,AIBDOT)
AIC = INTGRL(0.0,AICDOT)
BIA = INTGRL(0.0,BIADOT)
BIC = INTGRL(0.0,BICDOT)
CIA = INTGRL(0.0,CIADOT)
CIB = INTGRL(0.0,CIBDOT)
ARB = INTGRL(0.0,ARBDOT)
ARC = INTGRL(0.0,ARCDOT)
BRA = INTGRL(0.0,BRADOT)
BRC = INTGRL(0.0,BRCDOT)
```

```
    CRA = INTGRL(0.0,CRADOT)
    CRB = INTGRL(0.0,CRBDOT)
    SQAB = SQRT(AIB**2 + ARB**2)
    SQAC = SQRT(AIC**2 + ARC**2)
    SQBA = SQRT(BIA**2 + BRA**2)
    SQBC = SQRT(BIC**2 + BRC**2)
    SQCA = SQRT(CIA**2 + CRA**2)
    SQCB = SQRT(CIB**2 + CRB**2)
    TIMER FINTIM = 18.8
    PRTPLT YA, YB, YC. SQAB, SQAC, AQBA, SQBC, SQCA, SQCB
    END
    STOP
ENDJOB
```

Bibliography

[1] Berlin, M. Howard. *Design of Phase-Locked Loop Circuits, with experiments.* Indianapolis: Howard W. Sams & Co., Inc., 1978.

[2] K. Leentvaar and J. H. Flint. "The Capture Effect in FM Receivers," *IEEE Transactions on Communications*, Vol. COM-24, No. 5, pp. 195-199.May 1976.

[3] F. A. Cassara, H. Schachter, and R. Difazio. "Acquisition behavior of the cross-coupled phase-locked loop FM demodulator," *IEEE Transactions on Communications*, Vol. COM-28, pp.897-904. June 1980.

[4] Y. Bar-Ness, EE788, "Phase Locked Loops," class notes. New Jersey Institute of Technology, Spring 1990.

[5] Lindsey, Williams, C. *Phase Locked Loops.* New York: IEEE Press, pp1-25, 1986.

[6] Y. Bar-Ness, "Controlling the Feedback of Cross Coupled PLL by L.M.S. Cancelling Scheme." April 79. Private Communication.

[7] Y. Bar-Ness, F. A. Cassara, H. Schachter, and R. Difazio. "Cross Coupled Phase-Locked Loop with Closed Loop Amplitude Control," *IEEE Transactions on Communications*, Vol. COM-32, No. 2, pp. 531-539. February 1984.

[8] T. S. Sundrsh, F. A. Cassara, and H.Schachter. "Maximum a posteriori estimator for suppression of interchannel interference in FM receivers," *IEEE Transactions on Communications*, Vol. COM-25, pp.1480-1485. December 1977.

[9] Best, Roland. *Phase Locked Loops: Theory, Design, and Applications.* New York: McGraw-Hill, 1984.

[10] Viterbi, A. *Principles of Coherent Communication.* New York:McGraw-Hill, 1966.

[11] Blanchard, Alain. *Phase Locked Loops: Application to Coherent Receiver Design.* New York: John Willey & Sons, 1976.